High variation expected in the pace and burden of SARS-CoV-2 outbreaks across sub-Saharan Africa

Benjamin L. Rice[1,2], Akshaya Annapragada[3], Rachel E. Baker[1,4], Marjolein Bruijning[1], Winfred Dotse-Gborgbortsi[5], Keitly Mensah[6], Ian F. Miller[1], Nkengafac Villyen Motaze[7,8], Antso Raherinandrasana[9,10], Malavika Rajeev[1], Julio Rakotonirina[9,10], Tanjona Ramiadantsoa[11,12,13], Fidisoa Rasambainarivo[1,14], Weiyu Yu[15], Bryan T. Grenfell[1,16], Andrew J. Tatem[4], C. Jessica E. Metcalf[1,16]

Affiliations:

1. Department of Ecology and Evolutionary Biology, Princeton University, Princeton, NJ, USA
2. Madagascar Health and Environmental Research (MAHERY), Maroantsetra, Madagascar
3. Johns Hopkins University School of Medicine, Baltimore, MD, USA
4. Princeton Environmental Institute, Princeton University, Princeton, NJ, USA.
5. WorldPop, School of Geography and Environmental Science, University of Southampton, Southampton, UK
6. Centre population et Développement CEPED (Université de Paris), Institut Recherche et Développement, Paris, France
7. Centre for Vaccines and Immunology (CVI), National Institute for Communicable Diseases (NICD) a division of the National Health Laboratory Service (NHLS), South Africa
8. Department of Global Health, Faculty of Medicine and Health Sciences, Stellenbosch University, Cape Town, South Africa
9. Faculty of Medicine, University of Antananarivo, Madagascar
10. Institute of Public Health Analakely, Antananarivo, Madagascar
11. Department of Life Science, University of Fianarantsoa, Madagascar
12. Department of Mathematics, University of Fianarantsoa, Madagascar
13. Department of Integrative Biology, University of Wisconsin-Madison, WI, USA
14. Mahaliana Labs SARL, Antananarivo, Madagascar
15. School of Geography and Environmental Science, University of Southampton, Southampton, UK
16. Princeton School of Public and International Affairs, Princeton University, NJ 08450

Link to SSA-SARS-CoV-2 online tool: https://labmetcalf.shinyapps.io/covid19-burden-africa/

Correspondence: b.rice@princeton.edu

Abstract

A surprising feature of the SARS-CoV-2 pandemic to date is the low burdens reported in sub-Saharan Africa (SSA) countries relative to other global regions. Potential explanations (e.g., warmer environments[1], younger populations[2–4]) have yet to be framed within a comprehensive analysis accounting for factors that may offset the effects of climate and demography. Here, we synthesize factors hypothesized to shape the pace of this pandemic and its burden as it moves across SSA, encompassing demographic, comorbidity, climatic, healthcare and intervention capacity, and human mobility dimensions of risk. We find large scale diversity in probable drivers, such that outcomes are likely to be highly variable among SSA countries. While simulation shows that extensive climatic variation among SSA population centers has little effect on early outbreak trajectories, heterogeneity in connectivity is likely to play a large role in shaping the pace of viral spread. The prolonged, asynchronous outbreaks expected in weakly connected settings may result in extended stress to health systems. In addition, the observed variability in comorbidities and access to care will likely modulate the severity of infection: We show that even small shifts in the infection fatality ratio towards younger ages, which are likely in high risk settings, can eliminate the protective effect of younger populations. We highlight countries with elevated risk of ‘slow pace’, high burden outbreaks. Empirical data on the spatial extent of outbreaks within SSA countries, their patterns in severity over age, and the relationship between epidemic pace and health system disruptions are urgently needed to guide efforts to mitigate the high burden scenarios explored here.

The trajectory of the SARS-CoV-2 pandemic in lower latitude, lower income countries including in Sub-Saharan Africa (SSA) remains uncertain. To date, reported case counts and mortality in SSA have lagged behind other geographic regions: all SSA countries, with the exception of South Africa, reported less than 27,000 total cases as of June 2020 [5] (**Table S1**) - totals far less than observed in Asia, Europe, and the Americas [5,6]. However, recent increases in reported cases in many SSA countries make it unclear whether the relatively few reported cases to date indicate a reduced epidemic potential or rather an initial delay relative to other regions.

Correlation between surveillance capacity and case counts [7] obscure early trends in SSA (**Figure S1**). Experience from locations in which the pandemic has progressed more rapidly provides a basis of knowledge to assess the relative risk of populations in SSA and identify those at greatest risk. For example, individuals in lower socio-economic settings have been disproportionately affected in high latitude countries,[8,9] indicating poverty as an important determinant of risk. Widespread disruptions to routine health services have been reported [10–12] and are likely to be an important contributor to the burden of the pandemic in SSA [13]. The role of other factors from demography [2–4] to health system context [14] and intervention timing [15,16] is also increasingly well-characterized.

Factors expected to increase and decrease SARS-CoV-2 risk in SSA

Anticipating the trajectory of ongoing outbreaks in SSA requires considering variability in known drivers, and how they may interact to increase or decrease risk across populations in SSA and relative to non-SSA settings (**Figure 1**). For example, while most countries in SSA have ‘young’ populations, suggesting a decreased burden (since SARS-CoV-2 morbidity and mortality increase with age [2–4]), prevalent infectious and non-communicable comorbidities may counterbalance this demographic ‘advantage’ [14,17–19]. Similarly, SSA countries have health systems that vary greatly in their infrastructure, and dense, resource-limited urban populations may have fewer options for social distancing [20]. Yet, decentralized, community-based health systems that benefit from recent experience with epidemic response (e.g., to Ebola [21,22]) can be mobilized. Climate is frequently invoked as a potential mitigating factor for warmer and wetter settings [1], including SSA, but climate varies greatly between population centers in SSA and large susceptible populations may counteract any climate forcing during initial phases of the epidemic [23]. Connectivity, at international and subnational scales, also varies greatly [24,25] and the time interval between viral introductions and the onset of interventions such as lockdowns will modulate the trajectory [7]. Finally, burdens of malnutrition, infectious diseases, and many

other underlying health conditions are higher in SSA (**Table S2**), and their interactions with SARS-CoV-2 are, as of yet, poorly understood.

The highly variable social and health contexts of countries in SSA will drive location-specific variation in the magnitude of the burden, the time-course of the outbreak, and options for mitigation. Here, we synthesize the range of factors hypothesized to modulate the potential outcomes of SARS-CoV-2 outbreaks in SSA settings by leveraging existing data sources and integrating novel SARS-CoV-2 relevant mobility and climate-transmission models. Data on direct measures and indirect indicators of risk factors were sourced from publicly available databases including from the WHO, World Bank, UNPOP, DHS, GBD, and WorldPop, and newly generated data sets (see **Table S3** for details). We organize our assessment around two aspects that will shape national outcomes and response priorities in the event of widespread outbreaks: i) the burden, or expected severity of the outcome of an infection, which emerges from age, comorbidities, and health systems functioning, and ii) the rate of spread within a geographic area, or pace of the pandemic.

We group factors that may drive the relative rates of these two features (mortality burden and pace of the outbreak) along six dimensions of risk: (A) Demographic and socio-economic parameters related to transmission and burden, (B) Comorbidities relevant to burden, (C) Climatic variables that may impact the magnitude and seasonality of transmission, (D) Capacity to deploy prevention measures to reduce transmission, (E) Accessibility and coverage of existing healthcare systems to reduce burden, and (F) Patterns of human mobility relevant to transmission (**Table S2**).

National and subnational variability in SSA

National scale variability in SSA among these dimensions of risk often exceeds ranges observed across the globe (**Figure 2A-D**). For example, estimates of access to basic handwashing (i.e., clean water and soap [26]) among urban households in Mali, Madagascar, Tanzania, and Namibia (62-70%) exceed the global average (58%), but fall to less than 10% for Liberia, Lesotho, Congo DRC, and Guinea-Bissau (**Figure 2D**). Conversely, the range in the number of physicians is low in SSA, with all countries other than Mauritius below the global average (168.78 per 100,000 population) (**Figure 2A**). Yet, estimates are still heterogeneous within SSA, with, for example, Gabon estimated to have more than 4 times the physicians of neighboring Cameroon (36.11 and 8.98 per 100,000 population, respectively). This disparity is

likely to interact with social contact rates among the elderly in determining exposure and clinical outcomes (e.g., for variation in household size see **Figure 2E-F**). Relative ranking across variables is also uneven among countries with the result that this diversity cannot be easily reduced (e.g., the first two principal components explain only 32.6%, and 13.1% of the total variance as shown in **Figure S5**), motivating a more holistic approach to projecting burden.

Severity of infection outcome

To first evaluate variation in the burden emerging from the severity of infection outcome, we consider how demography, comorbidity, and access to care might modulate the age profile of SARS-CoV-2 morbidity and mortality [2–4]. Subnational variation in the distribution of high risk age groups indicates considerable variability, with higher burden expected in urban settings in SSA (**Figure 3A**), where density and thus transmission are likely higher [27].

Comorbidities and access to clinical care also vary across SSA (e.g., for diabetes prevalence and hospital bed capacity see **Figure 3B**). In comparison to settings where previous SARS-CoV-2 infection fatality ratio (*IFR*) estimates have been reported, mortality due to noncommunicable diseases in SSA increases more rapidly with age (**Figure S6**). Consequently, we explore scenarios where the SARS-CoV-2 *IFR* increases more rapidly with age than the baseline expected from other settings. Small shifts (e.g., of 2-10 years) in the *IFR* profile result in large effects on expected mortality for a given level of infection. For example, Chad, Burkina Faso, and the Central African Republic, while among the youngest SSA countries, have a relatively high prevalence of diabetes and relatively low density of hospital beds. A five year shift younger in the *IFR* by age profile of SARS-CoV-2 in these settings would result in nearly a doubling of mortality, to a rate that would exceed the majority of other, ‘older’ SSA countries at the unshifted baseline (**Figure 3C**, see supplement for details of methods). Although there is greater access to care in older populations by some metrics (**Figure 2A**, correlation between age and the number of physicians per capita, $r = 0.896$, $p < 0.001$), access to clinical care is highly variable overall (**Figure 3D**) and maps poorly to indicators of comorbidity (**Figure 3E**). Empirical data are urgently needed to assess the extent to which the *IFR*-age-comorbidity associations observed elsewhere are applicable to SSA settings with reduced access to advanced care. Yet both surveillance and mortality registration [28] are frequently under-resourced in SSA, complicating both evaluating and anticipating the burden of the pandemic, and underscoring the urgency of strengthening existing systems [22].

Pandemic pace

Next, we turn to the pace of the pandemic within each country. The frequency of viral introduction to each country, likely governed by international air travel in SSA [29], determines both the timing of the first infections and the number of initial infection clusters that can seed subsequent outbreaks. The relative importation risk among SSA cities and countries was assessed by compiling data from 108,894 flights arriving at 113 international airports in SSA from January to April 2020 (**Figure 4A**), stratified by the SARS-CoV-2 status at the departure location on the day of travel (**Figure 4B**). A small subset of SSA countries received a disproportionately large percentage (e.g., South Africa, Ethiopia, Kenya, Nigeria together contribute 47.9%) of the total travel from countries with confirmed SARS-CoV-2 infections, likely contributing to variation in the pace of the pandemic across settings [29,30].

Once local chains of infection are established, the rate of spread within countries will be shaped by efforts to reduce spread, such as handwashing (**Figure 2D**), population contact patterns including mobility and urban crowding [27] (e.g., **Figure 2C**), and potentially the effect of climatic variation [1]. Where countries fall across this spectrum of pace will shape interactions with lockdowns and determine the length and severity of disruptions to routine health system functioning.

Subnational connectivity varies greatly across SSA, both between subregions of a country and between cities and their rural periphery (e.g., as indicated by travel time to the nearest city over 50,000 population, **Figure 4C**). As expected, in stochastic simulations using estimates of viral transmission parameters and mobility (assuming no variation in control efforts, see methods), a smaller cumulative proportion of the population is infected at a given time in countries with larger populations in less connected subregions (**Figure 4D**). At the national level, susceptibility declines more slowly and more unevenly in such settings (e.g., Ethiopia, South Sudan, Tanzania) due to a lower probability of introductions and re-introductions of the virus locally; an effect amplified by lockdowns. It remains unclear whether the more prolonged, asynchronous epidemics expected in these countries or the overlapping, concurrent epidemics expected in countries with higher connectivity (e.g. Malawi, Kenya, Burundi) will be a greater stress to health systems. Outbreak control efforts are likely to be further complicated during prolonged epidemics if they intersect with seasonal events such as temporal patterns in human mobility [31] or other infections (e.g., malaria).

158 Turning to climate, despite extreme variation among cities in SSA (**Figure 4E**), large epidemic
159 peaks are expected in all cities (**Figure 4F**), even from models where transmission rate
160 significantly declines in warmer, more humid settings. In the absence of interventions, with
161 transmission rate modified by climate only, peak timing varies only by 4-6 weeks with peaks
162 generally expected earlier in more southerly, colder, drier, cities (e.g., Windhoek and Maseru)
163 and later in more humid, coastal cities (e.g., Bissau, Lomé, and Lagos). Apart from these slight
164 shifts in timing, large susceptible populations overwhelm the effects of climate [23], and earlier
165 suggestions that Africa's generally more tropical environment may provide a protective effect[1]
166 are not supported by evidence.
167
168 **Context-specific preparedness in SSA**
169 Our synthesis emphasizes striking country to country variation in drivers of the pandemic in SSA
170 (**Figure 2**), indicating variation in the burden (**Figure 3**) and pace (**Figure 4**) is to be expected
171 even across low income settings. As small perturbations in the age profile of mortality could
172 drastically change the national level burden in SSA (**Figure 3**), building expectations for the risk
173 for each country requires monitoring for deviations in the pattern of morbidity and mortality over
174 age. Transparent and timely communication of these context-specific risk patterns could help
175 motivate population behavioral changes and guide existing networks of community case
176 management.
177
178 Because the largest impacts of SARS-CoV-2 outbreaks may be through indirect effects on
179 routine health provisioning, understanding how existing programs may be disrupted differently
180 by acute versus longer outbreaks is crucial to planning resource allocation. For example,
181 population immunity will decline proportionally with the length of disruptions to routine
182 vaccination programs [31], resulting in more severe consequences in areas with prolonged
183 epidemic time courses.
184
185 Others have suggested that this crisis presents an opportunity to unify and mobilize across
186 existing health programs (e.g., for HIV, TB, Malaria, and other NCDs) [22]. While this may be a
187 powerful strategy in the context of acute, temporally confined crises, long term distraction and
188 diversion of resources [32] may be harmful in settings with extended, asynchronous epidemics. A
189 higher risk of infection among healthcare workers during epidemics [33,34] may amplify this risk.
190

Due to the lag relative to other geographic regions, many SSA settings retain the opportunity to prepare for and intervene in the earlier epidemic phases via context-specific deployment of both routine and pandemic related interventions. As evidenced by failures in locations where the epidemic progressed rapidly (e.g., USA), effective governance and management prior to reaching large case counts is likely to yield the largest rewards. Mauritius [35] and Rwanda [36], for example, have reported extremely low incidence thanks in part to a well-managed early response.

Conclusions

The burden and time-course of SARS-CoV-2 is expected to be highly variable across sub-Saharan Africa. As the outbreak continues to unfold, critically evaluating this mapping to better understand where countries lie in terms of their relative risk (e.g., see **Figure 5**) will require increased surveillance, and timely documentation of morbidity and mortality over age. Case counts are rising across SSA, but variability in testing regimes makes it difficult to compare observations to date with expectations in terms of pace (**Figure S7**). The potential to miss large clusters of cases (in contexts with weaker surveillance), combined with the potential that large areas remain unreached by the pandemic for longer (as a result of slower ‘pace’), indicate that immunological surveys are likely a powerful lens for understanding the landscape of population risk [37]. When considering hopeful futures with the possibility of a SARS-CoV-2 vaccine, it is imperative that vaccine distribution be equitable, and in proportion with need. Understanding factors that both drive spatial variation in vulnerable populations and temporal variation in pandemic progression could help approach these goals in SSA.

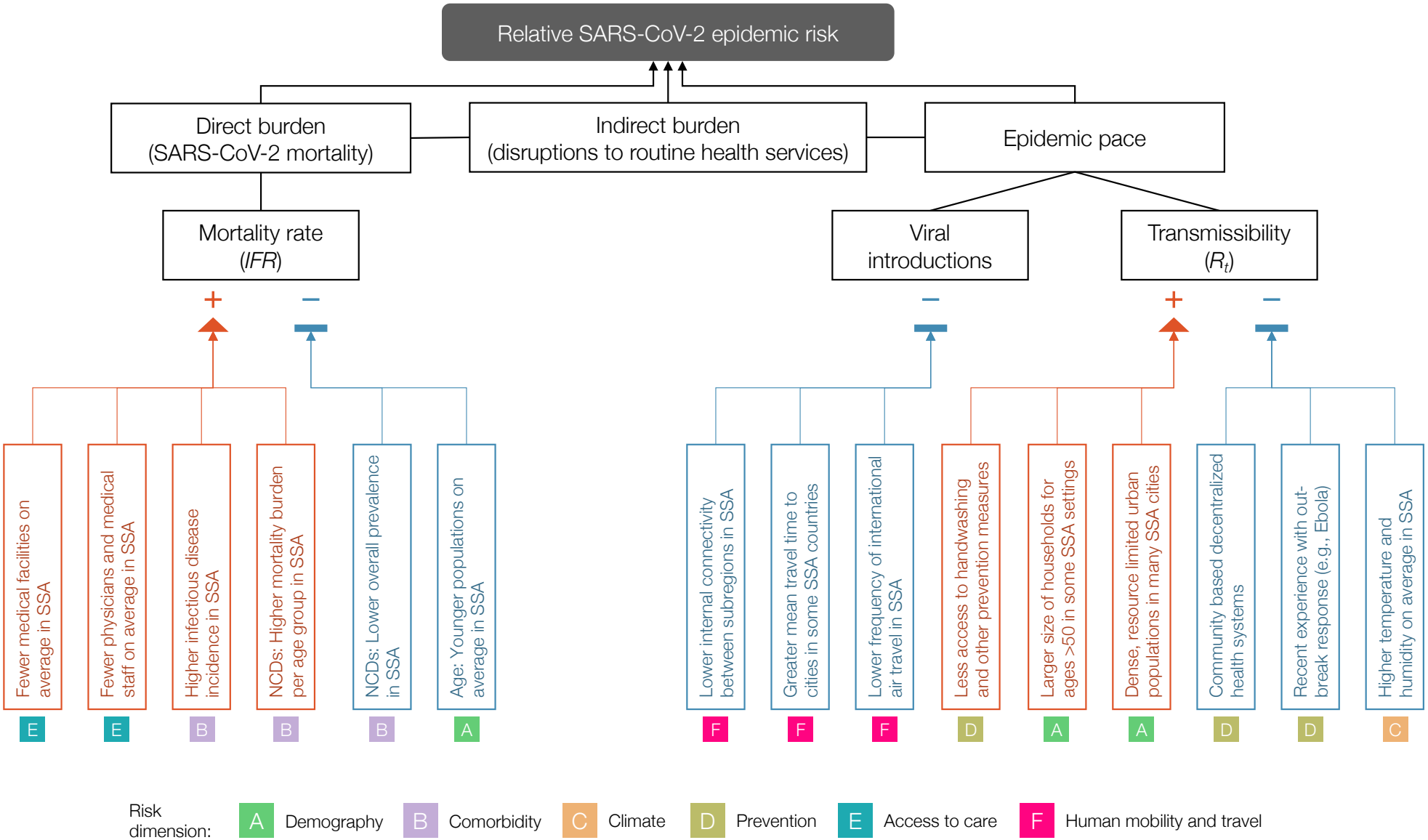

Figure 1 | Hypothesized modulators of relative SARS-CoV-2 epidemic risk in sub-Saharan Africa

Factors hypothesized to increase (red) or decrease (blue) mortality burden or epidemic pace within sub-Saharan Africa, relative to global averages, are grouped in six categories or dimensions of risk (A-F). In this framework, epidemic pace is determined by person to person transmissibility (which can be defined as the time-varying effective reproductive number, R_t) and introduction and geographic spread of the virus via human mobility.

SARS-CoV-2 mortality (determined by the infection fatality ratio, *IFR*) is modulated by demography, comorbidities (e.g., non-communicable diseases (NCDs)), and access to care. Overall burden is a function of direct burden and indirect effects due to, for example, disruptions in health services such as vaccination and infectious disease control. **Table S2** contains details and the references used as a basis to draw the hypothesized modulating pathways.

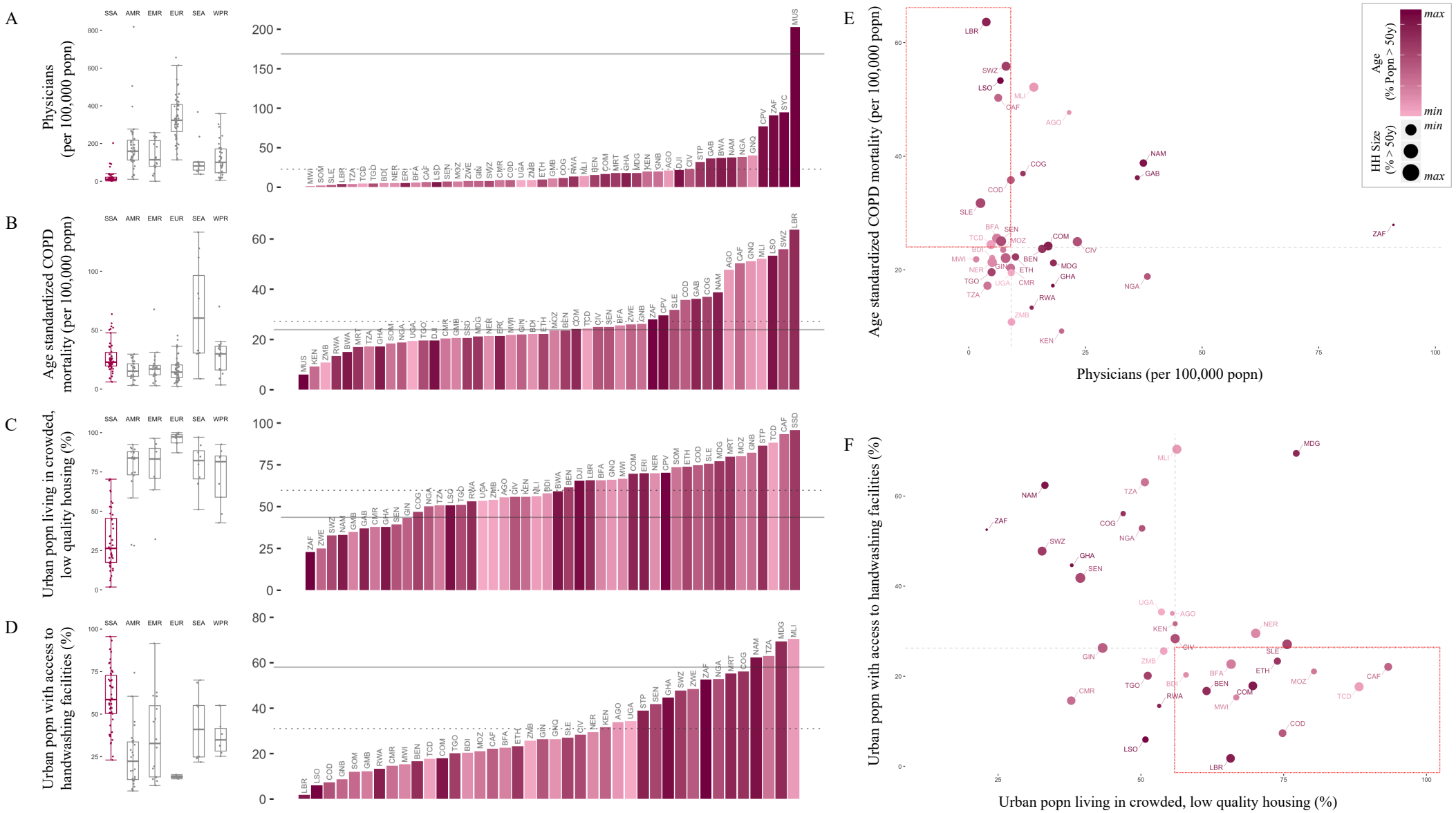

Figure 2 | Variation among sub-Saharan African countries in select determinants of SARS-CoV-2 risk

A-D: At right, SSA countries are ranked from least to greatest for each indicator; bar color shows population age structure (% of the population above age 50). Solid horizontal lines show the global mean value; dotted lines show the mean among SSA countries. At left, boxplots show median and interquartile range, grouped by geographic region, per WHO: sub-Saharan Africa (SSA); Americas Region (AMR); Eastern Mediterranean Region (EMR); Europe Region (EUR); Southeast Asia Region (SEA); Western Pacific Region (WPR).

E-F: Dot size shows mean household (HH) size for HHs with individuals over age 50; dashed lines show median value among SSA countries; quadrants of greatest risk are outlined in red (e.g., fewer physicians and greater age standardized Chronic Obstructive Pulmonary Disease (COPD) mortality). See Table S3, Figure S3, and the [SSA-SARS-CoV-2-tool] for full description and visualization of all variables.

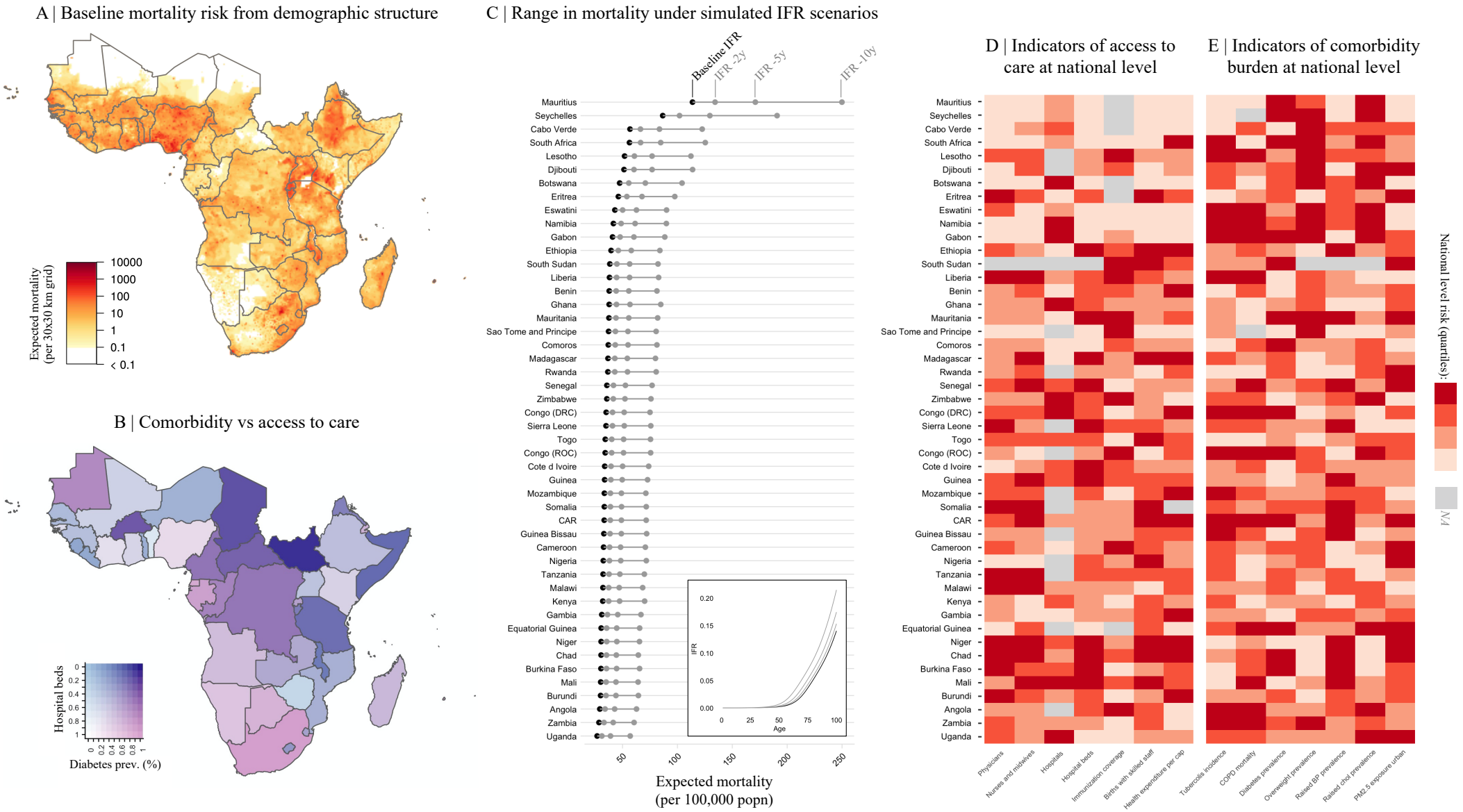

Figure 3 | Variation in expected burden for SARS-CoV-2 outbreaks in sub-Saharan Africa

A: Expected mortality in a scenario where cumulative infection reaches 20% across age groups and the infection fatality ratio (*IFR*) curve is fit to existing age-stratified *IFR* estimates (see methods, **Table S4**). **B**: National level variation in comorbidity and access to care variables, for e.g., diabetes prevalence among adults and the number of hospital beds per 100,000 population for sub-Saharan African countries. **C**: The range in mortality per 100,000 population expected in scenarios where cumulative infection rate is 20% and *IFR* per age is the baseline (black) or shifted 2, 5, or 10 years younger (gray). Inset, the *IFR* by age curves for each scenario.

D-E: Select national level indicators; estimates of reduced access to care (e.g., fewer hospitals) or increased comorbidity burden (e.g., higher prevalence of raised blood pressure) shown with darker red for higher risk quartiles (see **Figure S4** for all indicators). Countries missing data for an indicator (NA) are shown in gray. For comparison between countries, estimates are age-standardized where applicable (see **Table S3** for details). See the [SSA-SARS-CoV-2-tool] for high resolution maps for each variable and scenario.

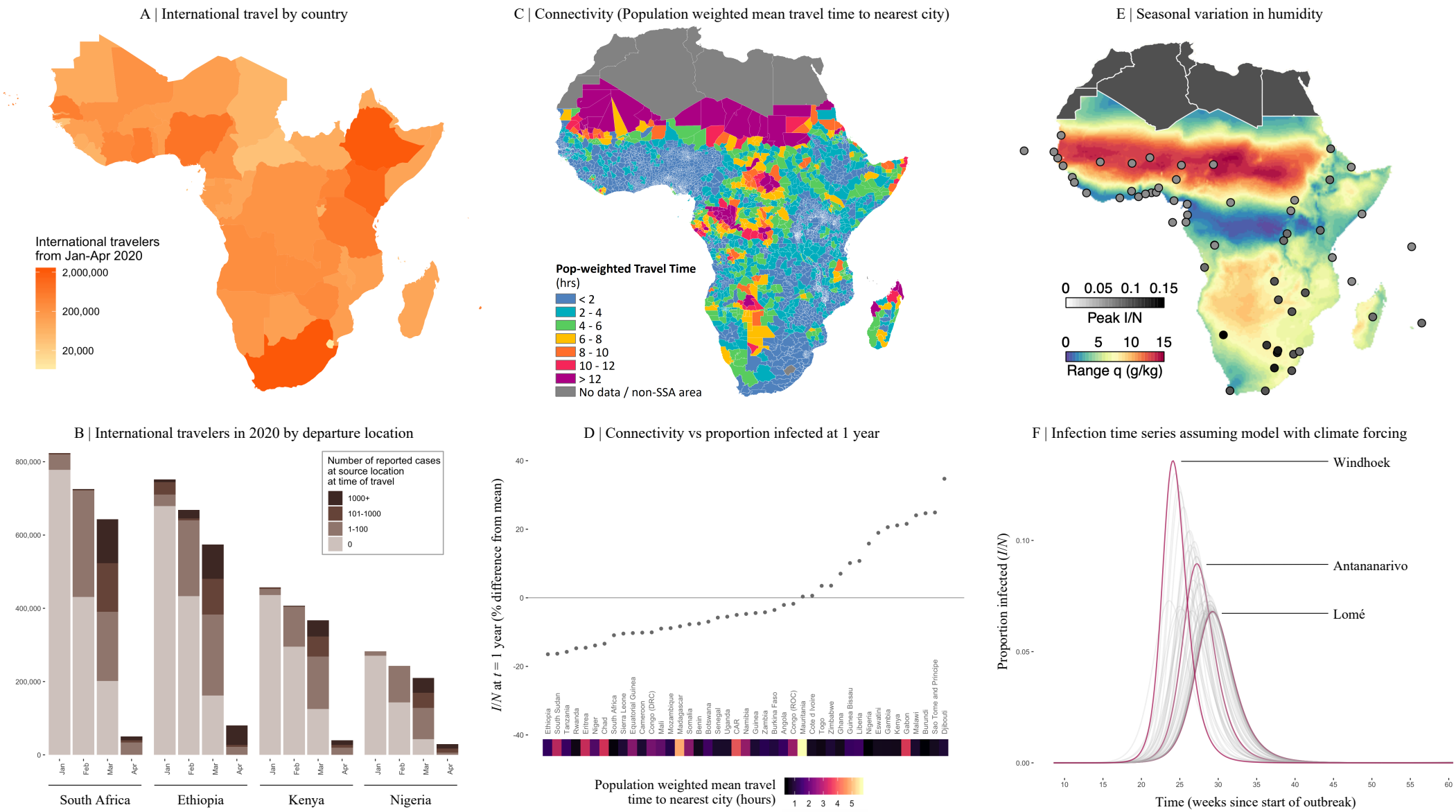

Figure 4 | Variation in connectivity and climate in sub-Saharan Africa and expected effects on SARS-CoV-2

A: International travelers to sub-Saharan Africa (SSA) from January to April 2020, as inferred from the number of passenger seats on arriving aircraft. **B**: For the four countries with the most arrivals, the proportion of arrivals by month coming from countries with 0, 1-100, 101-1000, and 1000+ reported SARS-CoV-2 infections at the time of travel (see **Table S5** for all others). **C**: Connectivity within SSA countries as inferred from average population weighted mean travel time to the nearest urban area greater than 50,000 population. **D**: Mean travel time at the national level and variation in the fraction of the population expected to be infected (*I/N*) in the first year from stochastic simulations (see methods). **E**: Climate variation across SSA as shown by seasonal range in specific humidity, *q* (g/kg) (max average *q* - min average *q*). Circles show peak proportion infected. **F:** The effect of local seasonality in SSA cities on outbreaks (*I/N* over time) in susceptible populations beginning in March 2020 (see methods).

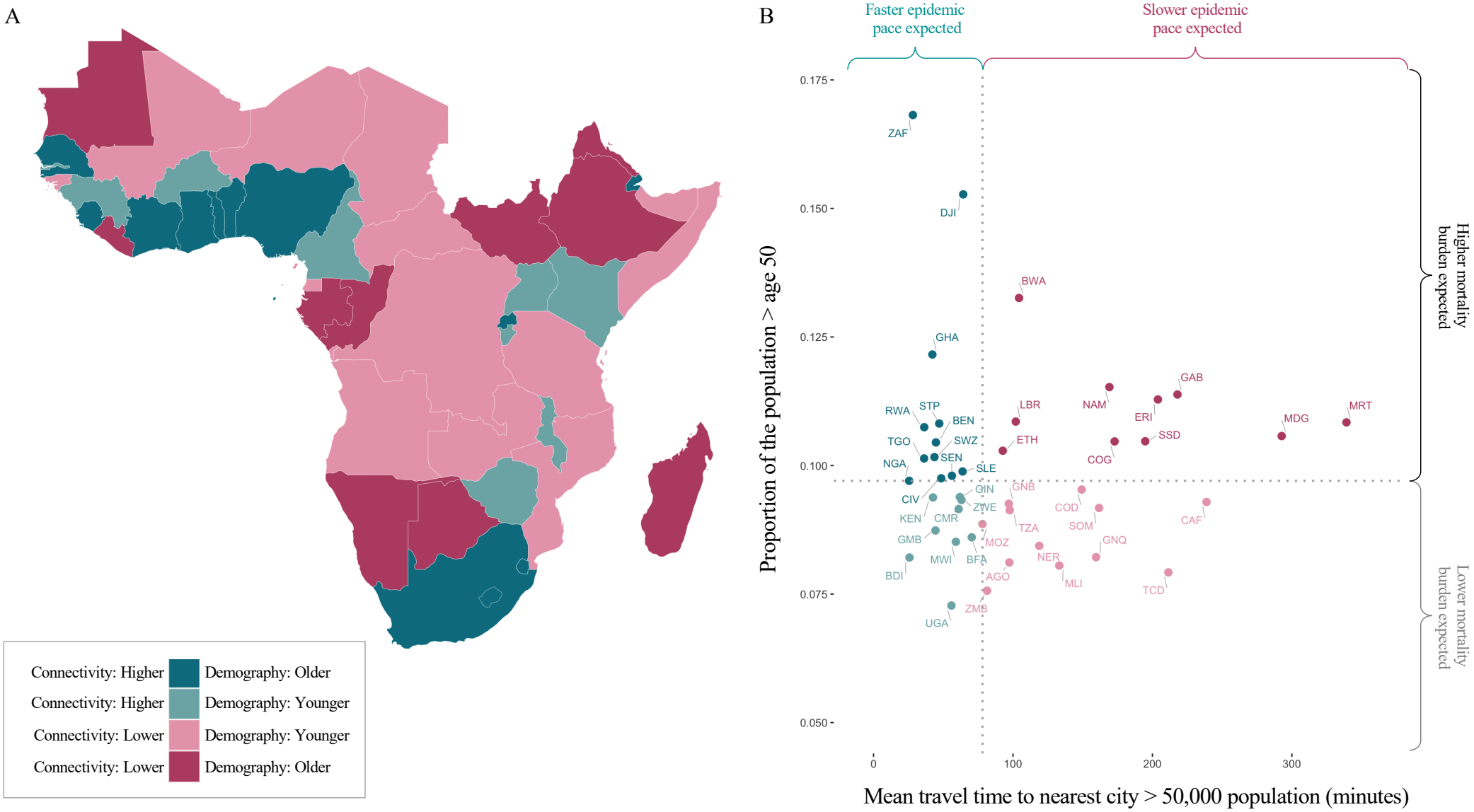

Figure 5 | Expected pace versus expected burden at the national level in SARS-CoV-2 outbreaks in sub-Saharan Africa

Countries are colored by with respect to indicators of their expected epidemic pace (using as an example subnational connectivity in terms of travel time to nearest city) and potential burden (using as an example the proportion of the population over age 50).
A: In pink, countries with less connectivity (i.e., less synchronous outbreaks) relative to the median among SSA countries; in blue, countries with more connectivity; darker colors show countries with older populations (i.e., a greater proportion in higher risk age groups).
B: Dotted lines show the median; in the upper right, in dark pink, countries are highlighted due to their increased potential risk for an outbreak to be prolonged (see metapopulation model methods) and high burden (see burden estimation methods).

Online Content

Methods, additional references, data, and detailed visualizations of variation in each of the variables and simulations can be accessed in the supplementary materials and online through an interactive tool [SSA-SARS-CoV-2-tool], which also contains code (in R).

Acknowledgements

REB is supported by the Cooperative Institute for Modeling the Earth System (CIMES). AA acknowledges support from the NIH Medical Scientist Training Program 1T32GM136577. AJT is funded by the BMGF (OPP1182425, OPP1134076 and INV-002697). MB is funded by NWO Rubicon grant 019.192EN.017.

Author contributions

Conceptualization: BLR, AA, REB, MB, WWD, KM, IFM, NVM, AR, MR, JR, TR, FR, WY, BTG, CJT, CJEM; *Data curation*: BLR, MR, MB, WWD, WY; *Formal analysis*: BLR, AA, MB, MR, REB; *Methodology*: BLR, MR, MB, REB, CJEM, BTG; *Software and Shiny app online tool*: BLR, MR, MB, REB, WY; *Visualization*: BLR, MR, MB, REB, WY; *Writing* – original draft: BLR, CJEM; *Writing – reviewing and editing*: BLR, AA, REB, MB, WWD, KM, IFM, NVM, AR, MR, JR, TR, FR, WY, BTG, CJT, CJEM

Additional Information

Supplementary Information is available for this paper. Correspondence and requests for materials should be addressed to BLR (b.rice@princeton.edu)

Data and materials availability

All materials are available in the online content

Competing interests

The authors declare no competing interests

Supplementary Materials Outline:

A1 Reported SARS-CoV-2 case counts, mortality, and testing in sub-Saharan Africa as of June 2020

Table S1: Sub-Saharan Africa country codes, case counts, and testing

Figure S1: Variation between SSA countries in testing and reporting rates

A2 Synthesizing factors hypothesized to increase or decrease SARS-CoV-2 epidemic risk in SSA

Table S2: Dimensions of risk and expected direction of effect on SARS-CoV-2 transmission or burden in sub-Saharan Africa (SSA) relative to higher latitude countries

Table S3: Variables and data sources

Figure S2: Year of most recent data available for variables compared between global regions

Figure S3: Variation among sub-Saharan African countries in determinants of SARS-CoV-2 risk by variable (a subset of variables is shown in Figure 2 in the main text)

Figure S4: Variation among sub-Saharan African countries in determinants of SARS-CoV-2 mortality risk by category (subsets of variables are shown in Figure 3 in the main text)

Data File 1: Data for all compiled indicators

A3 Principal component analysis (PCA) of variables considered

Figure S5: PCAs of all variables and category specific subsets of variables

Data File 2: GDP, GINI Index, and tests completed data for PCA visualizations

A4 Evaluating the burden emerging from the severity of infection outcome

Table S4: Sources of age-stratified infection fatality ratio (*IFR*) estimates

Figure S6: Age profiles of comorbidities in sub-Saharan Africa countries

A5 International air travel to sub-Saharan Africa

Table S5: Arrivals to SSA airports by the number of passenger seats and status of the SARS-CoV-2 pandemic at the origin at the time of travel

A6 Subnational connectivity among countries in sub-Saharan Africa

Metapopulation model methods

Figure S7: Pace of the outbreak

Figure S8: Cases and testing vs. the pace of the outbreak

A7 Modeling epidemic trajectories in scenarios where transmission rate depends on climate

Data on climate variation in SSA

Climate model methods

A1 | Reported SARS-CoV-2 case counts, mortality, and testing in sub-Saharan Africa as of June 2020

1.1. Variables and data sources for testing data

The numbers of reported cases, deaths, and tests for the 48 studied sub-Saharan Africa (SSA) countries (**Table S1**) were sourced from the Africa Centers for Disease Control (CDC) dashboard on June 30, 2020 (https://africacdc.org/covid-19/). Africa CDC obtains data from the official Africa CDC Regional Collaborating Centre and member state reports. Differences in the timing of reporting by member states results in some variation in recency of data within the centralized Africa CDC repository, but the data should broadly reflect the relative scale of testing and reporting efforts across countries.

The countries or member states within SSA in this study follow the United Nations and Africa CDC listed regions of Southern, Western, Central, and Eastern Africa (not including Sudan). From the Northern Africa region, Mauritania is included in SSA.

For comparison to non-SSA countries, the number of reported cases in other geographic regions were obtained from the Johns Hopkins University Coronavirus Resource Center on June 30, 2020 (https://coronavirus.jhu.edu/map.html).

Case fatality ratios (*CFR*s) were calculated by dividing the number of reported deaths by the number of reported cases and expressed as a percentage. Positivity was calculated by dividing the number of reported cases by the number of reported tests. Testing and case rates were calculated per 100,000 population using population size estimates for 2020 from the United Nations Population Division [38]. As reported confirmed cases are likely to be a significant underestimate of the true number of infections, *CFR*s may be a poor proxy for the infection fatality ratio (*IFR*), defined as the proportion of infections that result in mortality [4].

1.2 Variation in testing and mortality rates

Testing rates among SSA countries varied by multiple orders of magnitude: the number of tests completed per 100,000 population ranged from 6.50 in Tanzania to 13,508.13 in Mauritius (**Figure S1A**). The number of reported infections (i.e., positive tests) was strongly correlated with the number of tests completed (Pearson's correlation coefficient, $r = 0.9667$, $p < 0.001$) (**Figure S1B**). As of June 30, 2020, no deaths due to SARS-CoV-2 were reported to the Africa CDC for five SSA countries (Eritrea, Lesotho, Namibia, Seychelles, Uganda). Among countries with at least one reported death, *CFR* varied from 0.22% in Rwanda to 8.54% in Chad (**Figure S1C**). Limitations in the ascertainment of infection rates and the rarity of reported deaths (e.g., median number of reported deaths per SSA country was 25.5), indicate that the data are insufficient to determine country specific *IFR*s and *IFR* by age profiles. As a result, global *IFR* by age estimates were used for the subsequent analyses in this study.

Table S1

Sub-Saharan Africa country country codes, case counts, and testing as of June 30, 2020

Country Name	Country Code	Cases[a]	Deaths[a]	Tests[a]	Population[b]	Cases per 100k[c]	Tests per 100k[c]	Positivity (%)	CFR (%)
Angola	AGO	267	11	22895	32866268	0.81	69.66	1.17	4.12
Benin	BEN	1187	19	20014	12123198	9.79	165.09	5.93	1.60
Botswana	BWA	89	1	36868	2351625	3.78	1567.77	0.24	1.12
Burkina Faso	BFA	959	53	9040	20903278	4.59	43.25	10.61	5.53
Burundi	BDI	170	1	2359	11890781	1.43	19.84	7.21	0.59
Cameroon	CMR	12592	313	80000	26545864	47.43	301.37	15.74	2.49
Cabo Verde	CPV	1165	12	22665	555988	209.54	4076.53	5.14	1.03
Central Africa Republic	CAF	3429	45	23208	4829764	71.00	480.52	14.78	1.31
Chad	TCD	866	74	4633	16425859	5.27	28.21	18.69	8.55
Comoros	COM	293	7	1173	869595	33.69	134.89	24.98	2.39
Côte d'Ivoire	CIV	9101	66	48340	26378275	34.50	183.26	18.83	0.73
Congo (DRC)	COD	6939	167	24657	89561404	7.75	27.53	28.14	2.41
Djibouti	DJI	4656	53	46108	988002	471.25	4666.79	10.10	1.14
Equatorial Guinea	GNQ	2001	32	16000	1402985	142.62	1140.43	12.51	1.60
Eritrea	ERI	191	0	7943	3546427	5.39	223.97	2.40	0.00
Eswatini	SWZ	781	11	11094	1160164	67.32	956.24	7.04	1.41
Ethiopia	ETH	5846	103	250604	114963583	5.09	217.99	2.33	1.76
Gabon	GAB	5209	40	34774	2225728	234.04	1562.37	14.98	0.77
Gambia	GMB	45	2	2947	2416664	1.86	121.94	1.53	4.44
Ghana	GHA	17351	112	294867	31072945	55.84	948.95	5.88	0.65
Guinea	GIN	5291	30	33737	13132792	40.29	256.89	15.68	0.57
Guinea Bissau	GNB	1614	21	8056	1967998	82.01	409.35	20.03	1.30
Kenya	KEN	6190	144	167417	53771300	11.51	311.35	3.70	2.33
Lesotho	LSO	27	0	3000	2142252	1.26	140.04	0.90	0.00
Liberia	LBR	768	34	6125	5057677	15.18	121.10	12.54	4.43

48 (Table S1 continued)

Country Name	Country Code	Cases[a]	Deaths[a]	Tests[a]	Population[b]	Cases per 100k[c]	Tests per 100k[c]	Positivity (%)	CFR (%)
Madagascar	MDG	2138	20	21444	27691019	7.72	77.44	9.97	0.94
Malawi	MWI	1152	13	13369	19129955	6.02	69.89	8.62	1.13
Mali	MLI	2147	113	12869	20250834	10.60	63.55	16.68	5.26
Mauritania	MRT	4149	126	39398	4649660	89.23	847.33	10.53	3.04
Mauritius	MUS	341	10	171792	1271767	26.81	13508.13	0.20	2.93
Mozambique	MOZ	859	5	28586	31255435	2.75	91.46	3.00	0.58
Namibia	NAM	183	0	8706	2540916	7.20	342.63	2.10	0.00
Niger	NER	1074	67	6555	24206636	4.44	27.08	16.38	6.24
Nigeria	NGA	24567	565	130164	206139587	11.92	63.14	18.87	2.30
Congo (ROC)	COG	1245	40	11790	5518092	22.56	213.66	10.56	3.21
Rwanda	RWA	900	2	137751	12952209	6.95	1063.53	0.65	0.22
São Tomé and Príncipe	STP	713	13	17773	219161	325.33	8109.56	4.01	1.82
Senegal	SEN	6698	108	76343	16743930	40.00	455.94	8.77	1.61
Seychelles	SYC	77	0	704	98340	78.30	715.88	10.94	0.00
Sierra Leone	SLE	1427	60	9973	7976985	17.89	125.02	14.31	4.20
Somalia	SOM	2894	90	11807	15893219	18.21	74.29	24.51	3.11
South Africa	ZAF	138134	2456	1567084	59308690	232.91	2642.25	8.81	1.78
South Sudan	SSD	2006	37	10630	11193729	17.92	94.96	18.87	1.84
Tanzania	TZA	509	21	3880	59734213	0.85	6.50	13.12	4.13
Togo	TGO	642	14	30316	8278737	7.75	366.19	2.12	2.18
Uganda	UGA	870	0	186200	45741000	1.90	407.07	0.47	0.00
Zambia	ZMB	1531	21	53370	18383956	8.33	290.31	2.87	1.37
Zimbabwe	ZWE	567	6	66712	14862927	3.81	448.85	0.85	1.06

49

50 [a] Data from Africa CDC as of June 30, 2020 (https://africacdc.org/covid-19/)

51 [b] Data from UN Population Division UNPOP (2019 revision) estimates of population by single calendar year (2020)[38]

52 [c] Rates per 100,000 population

53

Figure S1

Variation between SSA countries in testing and reporting rates as of June 30, 2020

A: Reported number of tests completed per country as of June 2020 (source: Africa CDC). **B**: Number of infections (I) per reported number of tests (T); line shows linear regression: $I = 8.454\times10^{-2}\times T - 8.137\times10^{2}$ ($R^2 = 0.933$, $p < 0.001$).

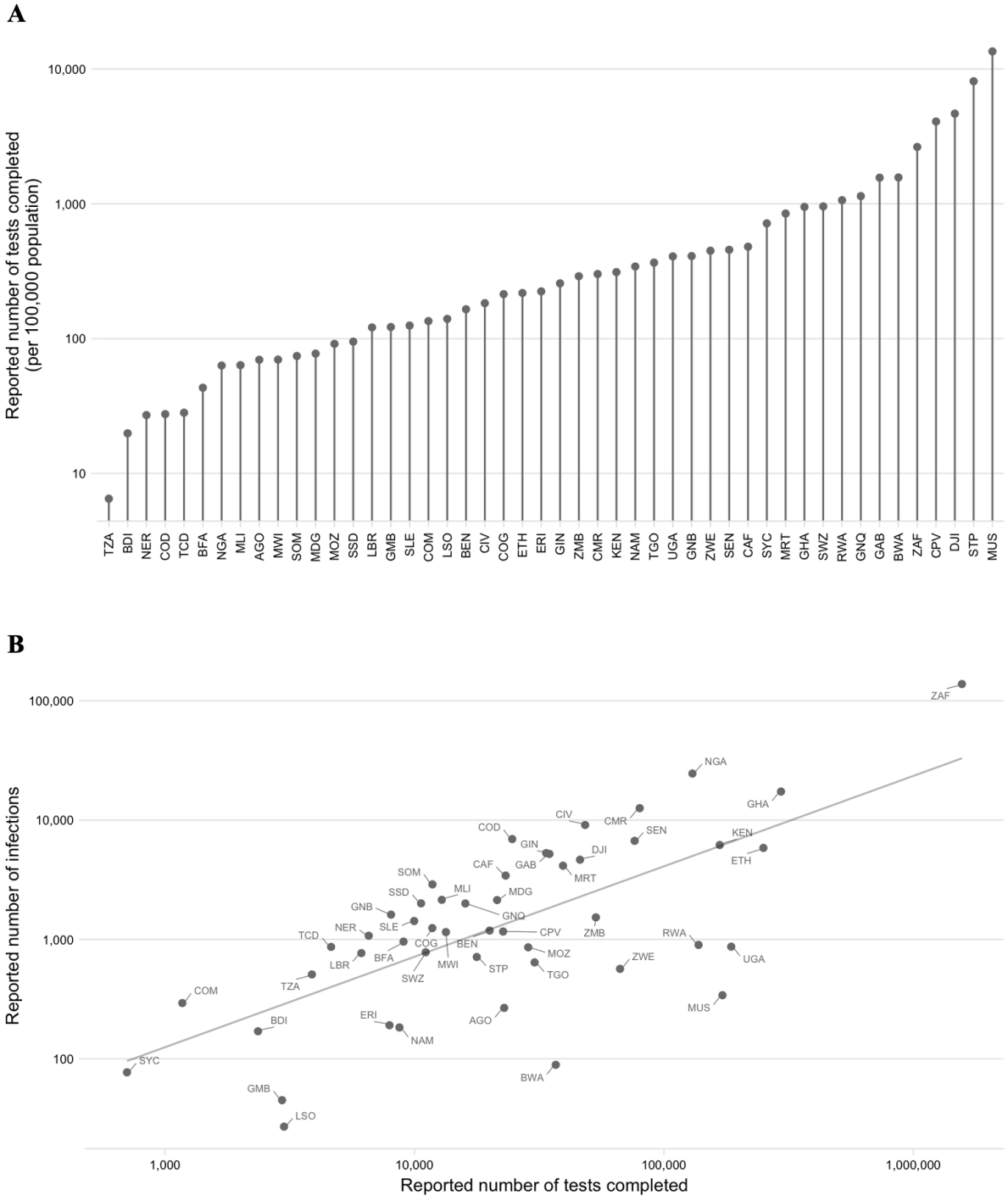

(Figure S1 continued)
C: Reported infections and deaths for sub-Saharan African countries with case fatality ratios (*CFR*s) shown as diagonal lines. **D**: Date of first detection per number of reported tests

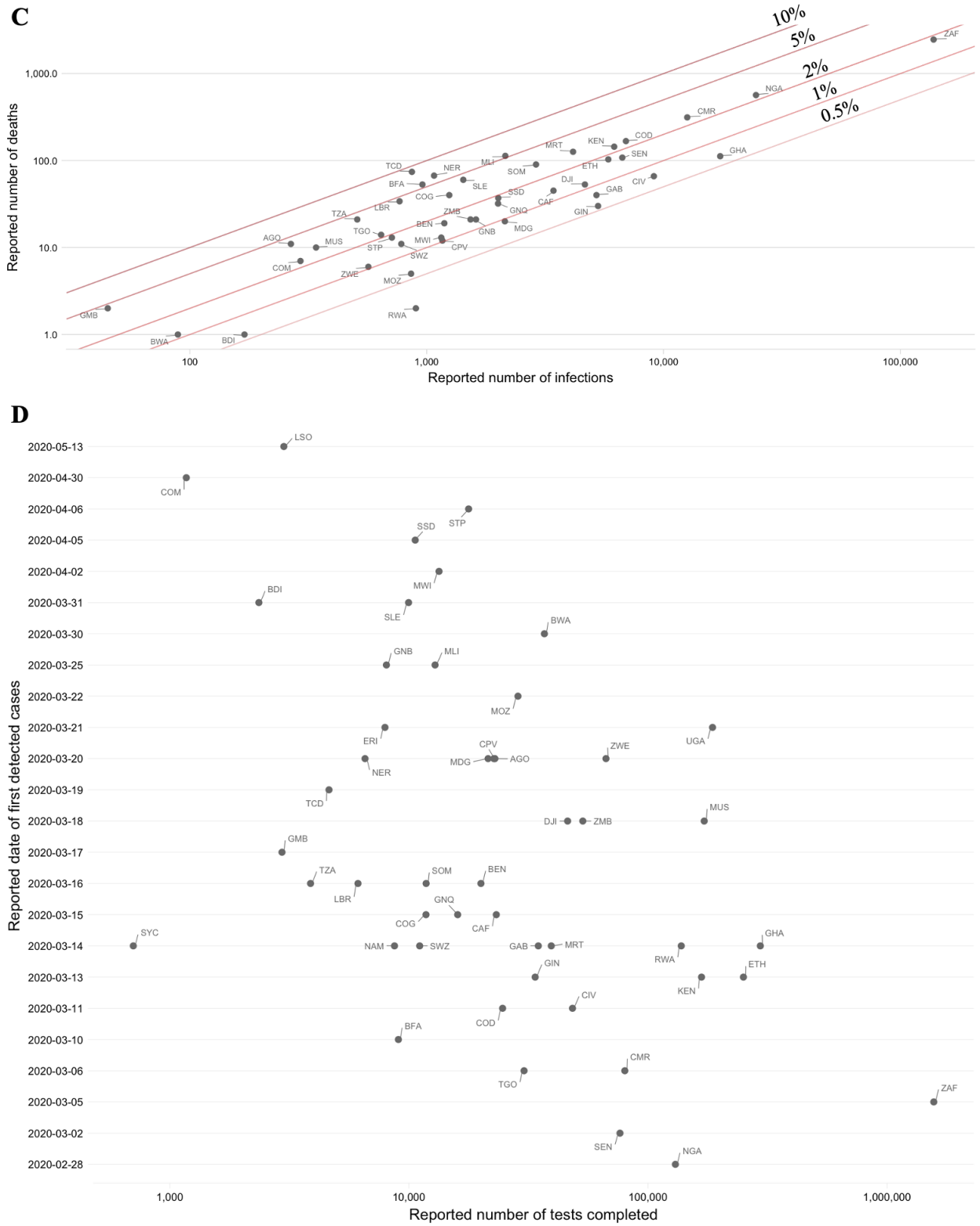

A2 | Methods: Synthesizing factors hypothesized to increase or decrease SARS-CoV-2 epidemic risk in SSA

2.1. Variable selection and data sources for variables hypothesized to associate with an increased probability of severe clinical outcomes for an infection

To characterize epidemic risk, defined as potential SARS-CoV-2 related morbidity and mortality, we first synthesized factors hypothesized to influence risk in SSA settings (**Table S2**). Early during the pandemic, evidence suggested that age was an important risk factor associated with morbidity and mortality associated with SARS-CoV-2 infection [39], a pattern subsequently confirmed across settings [2,9,40]. Associations between SARS-CoV-2 mortality and comorbidities including hypertension, diabetes, and cardiovascular disease emerged early [39]; and have been observed across settings, with further growing evidence for associations with obesity [9,41], severe asthma [9], and respiratory effects of pollution [42].

Many possible sources of bias complicate interpretation of these associations [43], and while they provide a useful baseline, inference is also likely to change as the pandemic advances. To reflect this, our analysis combines a number of high level variables likely to broadly encompass these putative risk factors (e.g., non-communicable disease (NCD) related mortality and health life expectancy) with more specific measures encompassed in evidence to date (e.g., prevalence of diabetes, obesity, and respiratory illness such as Chronic Obstructive Pulmonary Disease (COPD)). We also include measures relating to infectious diseases, undernourishment, and anemia given their interaction and effects in determining health status in these settings [44].

Data on the identified indicators were sourced in May 2020 from the World Health Organization (WHO) Global Health Observatory (GHO) database (https://www.who.int/data/gho), World Bank (https://data.worldbank.org/), and other sources detailed in **Table S3**. National level demographic data (population size and age structure) was sourced from United Nations World Population Prospects (UNPOP) [38] and data on subnational variation in demography was sourced from WorldPop [25]. Household size data was defined by the mean number of individuals in a household with at least one person aged > 50 years, taken from the most recently available demographic health survey (DHS) data [45]. All country level data for all indicators can be found online at the [SSA-SARS-CoV-2-tool]).

Comparisons of national level estimates sourced from WHO and other sources are affected by variation within countries and variation in the uncertainty around estimates from different geographical areas. To assess potential differences in data quality between geographic areas we compared the year of most recent data for variables (**Figure S2**). The mean (range varied from 2014.624 to 2014.928 by region) and median year (2016 for all regions) of the most recent data varied little between regions. To account for uncertainty associated in the estimates available for a single variable, we also include multiple variables per category (e.g., demographic and socio-economic factors, comorbidities, access to care) to avoid reliance on a single metric. This allows exploring variation between countries across a broad suite of variables likely to be indicative of the different dimensions of risk.

Although including multiple variables that are likely to be correlated (see PCA methods below for further discussion) would bias inference of cumulative risk in a statistical framework, we do not attempt to quantitatively combine risk across variables for a country, nor project risk based on the variables included here. Rather, we characterize the magnitude of variation among countries for these variables (see **Figure 2** in the main text for a subset of the variables; **Figure 3B** for bivariate risk maps following [46]) and then explore the range of outcomes that would be expected under scenarios where *IFR* increases with age at different rates (see **Figure 3** in the main text).

2.2. Variable selection and data sources for variables hypothesized to modulate the rate of viral spread

In addition to characterizing variation among factors likely to modulate burden, we also synthesize data sources relevant to the rate of viral spread, or pace, for the SARS-CoV-2 pandemic in SSA. Factors hypothesized to modulate viral transmission and geographic spread include climatic factors (e.g., specific humidity), access to prevention measures (e.g., handwashing), and human mobility (e.g., international and domestic travel). **Table S2** outlines the dimensions of risk selected and references the previous studies relevant to the selection of these factors.

Climate data was sourced from the global, gridded ERA5 dataset [47] where model data is combined with global observation data (see **Section A7** for details).

International flight data was obtained from a custom report from OAG Aviation Worldwide (UK) and included the departure location, airport of arrival, date of travel, and number of passenger seats for flights arriving to 113 international airports in SSA (see **Section A5**).

As an estimate of connectivity within subregions of countries, the population weighted mean travel time to the nearest city with a population greater than 50,000 was determined; details are provided in **Section A6**. To obtain a set of measures that broadly represent connectivity within different countries in the region, friction surfaces from ref[24] were used to obtain estimates of the connectivity between different administrative level 2 units within each country. Details of this, alongside the metapopulation model framework used to simulate viral spread with variation in connectivity are in **Section A6**.

Figure 2 in the main text shows variation among SSA countries for four of the variables; **Figure S3** shows variation for all variables. **Figure 3** in the main text shows variation for a subset of the comorbidity and access to care indicators as a heatmap; **Figure S4** shows variation for all the variables (both also available online at the [SSA-SARS-CoV-2-tool]).

149 **Table S2**

150 **Hypothesized dimensions of risk and expected direction of effect on SARS-CoV-2**
151 **transmission or burden in sub-Saharan Africa (SSA) relative to higher latitude countries**

Dimension of risk	Factors hypothesized to **decrease** transmission or burden in sub-Saharan Africa relative to other geographic areas	Factors hypothesized to **increase** transmission or burden in sub-Saharan Africa relative to other geographic areas
(A) Demographic and socio-economic characteristics in SSA	Younger populations, and thus a smaller proportion of individuals in the older age groups that experience the highest mortality [2–4]	A larger proportion of urban populations living in dense settings, which may result in higher transmission [48]; higher contact with older individuals as a result of multi-generation households [14]
(B) Comorbidities in SSA	Lower rates of some comorbidities that have been associated with risk of worse outcomes, e.g., obesity [9,41]	Higher rates of NCDs such as hypertension or COPD[39], which are associated with worse outcomes; and a potential role for as yet undescribed interactions e.g., with anemia, or high prevalence infectious diseases
(C) Climate in SSA	Warmer, wetter climates on average driving reduced transmission [1,49]	
(D) Capacity to deploy prevention measures in SSA	Experience with previous outbreak response which may yield more rapid and nimble approaches to reducing transmission [21,22]	Lower access to handwashing [50,51] and other prevention options such as self-isolation [52], increasing transmission
		Subregions of countries with reduced governance infrastructure [53]
(E) Access to healthcare in SSA		Larger variation in access to and coverage of health systems [54] including fewer medical staff and facilities such as hospital beds [14] increasing burden
		Increased vulnerability to disruption of routine health services (e.g.,[31])
		Limited testing capacity [55] reducing the capacity to identify and interrupt chains of transmission
(F) Human mobility and travel in SSA	Fewer viral importations due to reduced frequency of international travel [29,30]	
	Decreased rate of internal spread due to less connectivity within countries [56]	

152

153 # Table S3

154 **Variables and data sources for indicators of SARS-CoV-2 epidemic risk in sub-Saharan**
155 **Africa**

ID	Variable	Source	Hypothesized association(s) with SARS-CoV-2 outcomes
(A) Demographic and socio-economic characteristics			
A1	Human population size; Proportion of population over age 50 (%) from the UN Population Division UNPOP (2019 revision) estimates of population by single calendar year (2020), age, and country	UN[38]	Morbidity and mortality observed to increase with age (e.g, [2–4])
A2	Subnational spatial variation in the distribution of the human population and age structure	WorldPop	
A3	Household size: Mean household size for households with an individual over age 50	DHS	Proxy for social contact rate for the elderly population at higher risk for SARS-CoV-2 morbidity and mortality [14]
A4	Proportion of households with an individual over age 50	DHS	
A5	Health life expectancy (HALE) at age 60 (years)	WHO	Proxy for baseline health status of elderly population
A6	Proportion of population below the poverty line (%)	World Bank	More severe clinical outcomes associated with poverty; A proxy for access to advanced care [57,58]
A7	Proportion of the urban population living in crowded, low quality housing (defined as households lacking one or more of the following conditions: access to improved water, access to improved sanitation, sufficient living area, and durability of housing) (%)	World Bank	Indicator of capacity for prevention (e.g., through handwashing); Transmission observed to increase with crowding [48]
A8	Gross domestic product (GDP) per capita	World Bank	Used in PCA analysis (see below) as an indicator of socio-economic status at the national level
A9	GINI index, a measure of inequality in the distribution of income	World Bank	
(B) Comorbidities: General and nutrition related non-communicable diseases (NCDs)			
B1	NCDs overall mortality per 100 000 popn, age-standardized	WHO	Indicator of NCD burden in population; Comorbidities increase probability of severe clinical outcomes
B2	Cardiovascular disease related mortality per age group (annual deaths attributable per 100,000 population)	GDB 2017[59]	
B3	Diabetes prevalence among ages 20-79 (%)	World Bank	Increases probability of severe clinical outcomes
B4	Diabetes related mortality per age group (annual deaths attributable per 100,000 population)	GDB 2017[59]	

156
157
158
159

160
161 (Table S3 continued)

ID	Variable	Source	Hypothesized association(s) with SARS-CoV-2 outcomes
(B) Comorbidities: General and nutrition related non-communicable diseases (NCDs)			
B5	Raised glucose prevalence, age-standardized (%)	WHO	Indicator of metabolic disease risk; Metabolic disease increases probability of severe clinical outcomes
B6	Raised blood pressure prevalence, age-standardized (%)	WHO	
B7	Raised cholesterol prevalence, age-standardized (%)	WHO	
B8	Overweight prevalence among adults, age-standardized (%)	WHO	
B9	Anemia prevalence among non-pregnant women (%)	WHO	Indicator of poor nutritional status; Poor nutritional status may increase probability of severe clinical outcomes
B10	Undernourishment prevalence (%)	WHO	
(B) Comorbidities: NCDs related to respiratory system and pollution			
B11	Annual mean PM2.5 exposure in urban areas (ug/m3)	WHO	Exposure to air pollution increases mortality [42]
B12	Lung, tracheal, and esophageal cancer mortality per 100 000 popn, age-standardized	WHO	Indicator of prevalence and management of chronic disease and inflammation affecting the respiratory tract
B13	Chronic respiratory diseases (excluding asthma) related mortality per age group (annual deaths attributable per 100,000 population)	GDB 2017[59]	
B14	COPD mortality per 100 000 popn, age-standardized	WHO	
(B) Comorbidities: Infectious diseases			
B15	Respiratory infections mortality per 100 000 popn, age-standardized	WHO	Indicator of prevalence and management of infectious disease affecting the respiratory tract
B16	TB incidence per 100 000 popn	World Bank	Indicator of susceptibility to respiratory infections and immune suppression
B17	HIV prevalence among ages 15-49 (%)	World Bank	Indicator of immunosuppressed population
(C) Climate			
C1	Seasonal change in specific humidity (in selected urban centers)	ERA5[47]	Transmission rate of coronaviruses may decline with humidity
(D) Capacity to deploy prevention measures			
D1	Proportion of urban popn with basic handwashing facilities with water and soap at home (%)	WHO	Handwashing observed to reduce infection rates for respiratory pathogens

D2	Proportion of the population with access to a handwashing station with soap and water in 2019	Ref[60]	

(Table S3 continued)

ID	Variable	Source	Hypothesized association(s) with SARS-CoV-2 outcomes
(D) Capacity to deploy prevention measures			
D3	Proportion of 1 year olds receiving full immunization coverage (%)	WHO	Proxy for coverage of routine health services
D4	Reported number of completed tests reported for SARS-CoV-2 infection as of June 30, 2020	Africa CDC	Indicator of surveillance capacity
(E) Access to healthcare in SSA			
E1	Proportion of children with pneumonia symptoms taken to a health facility (%)	WHO	Proxy for access to medical care and care seeking
E2	Subnational spatial variation in the probability of seeking treatment for fever at public facilities	Ref[61]	
E3	Proportion of births attended by skilled staff (%)	World Bank	
E4	Nurses and midwives per 100 000 popn	World Bank	Indicators of treatment capacity
E5	Physicians per 100 000 popn	World Bank	
E6	Hospitals per 100 000 popn	World Bank	
E7	Hospital beds 100 000 popn	World Bank	
E8	Health expenditure per capita in (USD)	WHO	Proxy for health system resources; A significant predictor of intensive care unit (ICU) capacity [62]
E9	Proportion of health expenditures that are out-of-pocket (%)	WHO	
(F) Human mobility and travel: International			
F1	Estimated number of international passengers arriving at SSA airports from January-April 2020	OAG	Indicator of the timing and number of introductions of SARS-CoV-2
F2	Estimated number of international passengers arriving at SSA airports from January-April 2020 by SARS-CoV-2 status at departure location	OAG	

166 (Table S3 continued)

ID	Variable	Source	Hypothesized association(s) with SARS-CoV-2 outcomes
(F) Human mobility and travel: Domestic			
F3	National population-weighted mean travel time to the nearest city (national mean of indicator F4)	Ref[63]	Indicator of connectivity within countries; A proxy for the rate of human mobility
F4	Population-weighted mean travel time to the nearest city (population > 50,000) for administrative level 2 units	Ref[63]	
F5	Relative costs of travel between centroids of administrative level 2 derived from friction surfaces obtained by integrating data on travel infrastructure (Open Street Map, land cover types, etc).	Ref[24]	

167

Figure S2

Year of most recent data available for variables compared between global regions

Dotted vertical line shows regional median; solid vertical line shows regional mean. Note that most data comes from 2015-2019 (median = 2016, mean = 2014.624-2014.928).

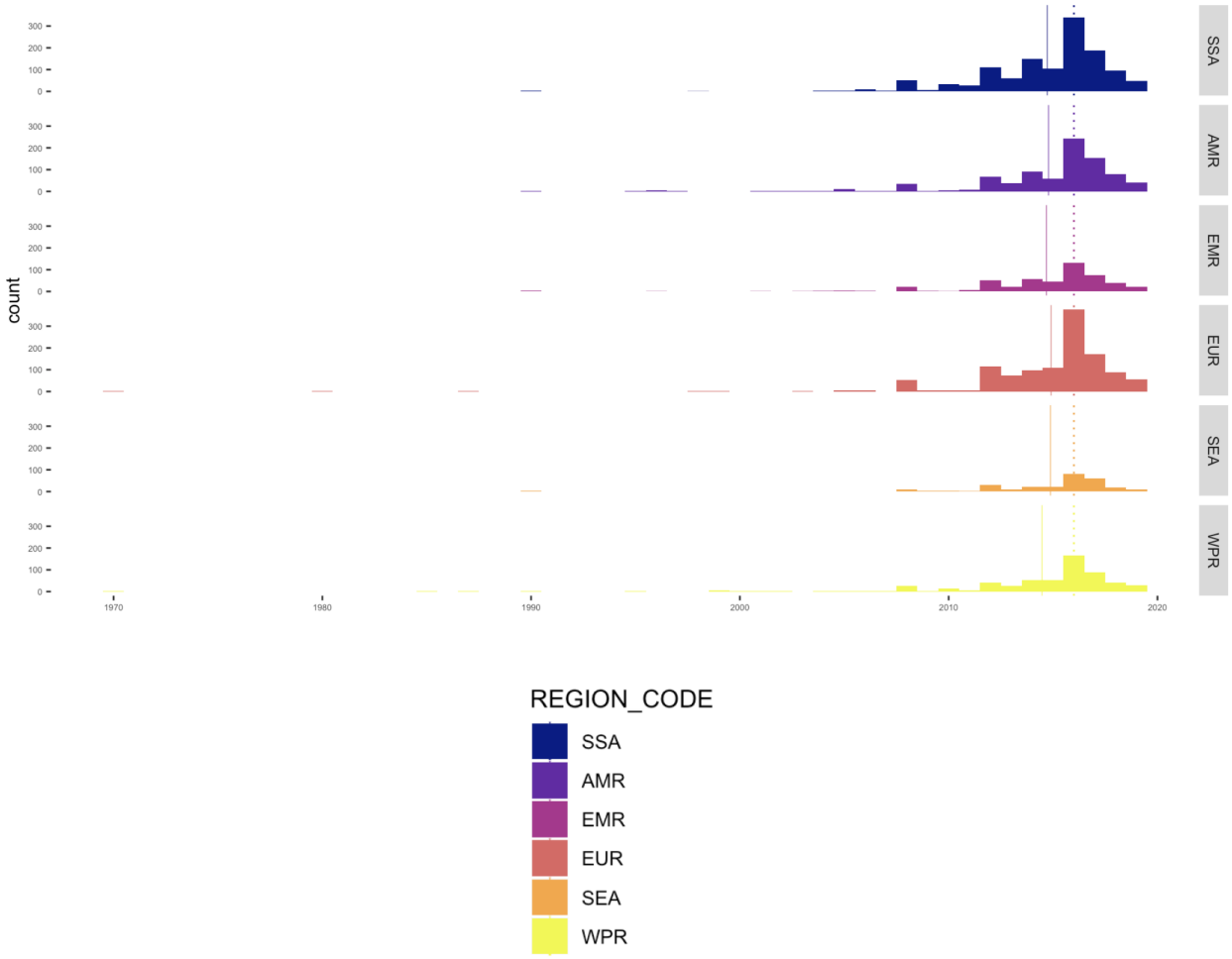

Figure S3

Variation among sub-Saharan African countries in determinants of SARS-CoV-2 risk by variable

A subset of variables is shown in Figure 2A-D in the main text, the remaining variables are shown in supplementary file “Figure S3 compiled.pdf” and available online: [SSA-SARS-CoV-2-tool]

Figure S4

Variation among sub-Saharan African countries in determinants of SARS-CoV-2 mortality risk by category

A subset of variables is shown in Figure 3D-E in the main text, the remaining variables are shown and available online: [SSA-SARS-CoV-2-tool]

A: Select national level indicators; estimates of increased comorbidity burden (e.g., higher prevalence of raised blood pressure) shown with darker red for higher risk quartiles Countries missing data for an indicator (NA) are shown in gray. For comparison between countries, estimates are age-standardized where applicable (see **Table S3** for details)

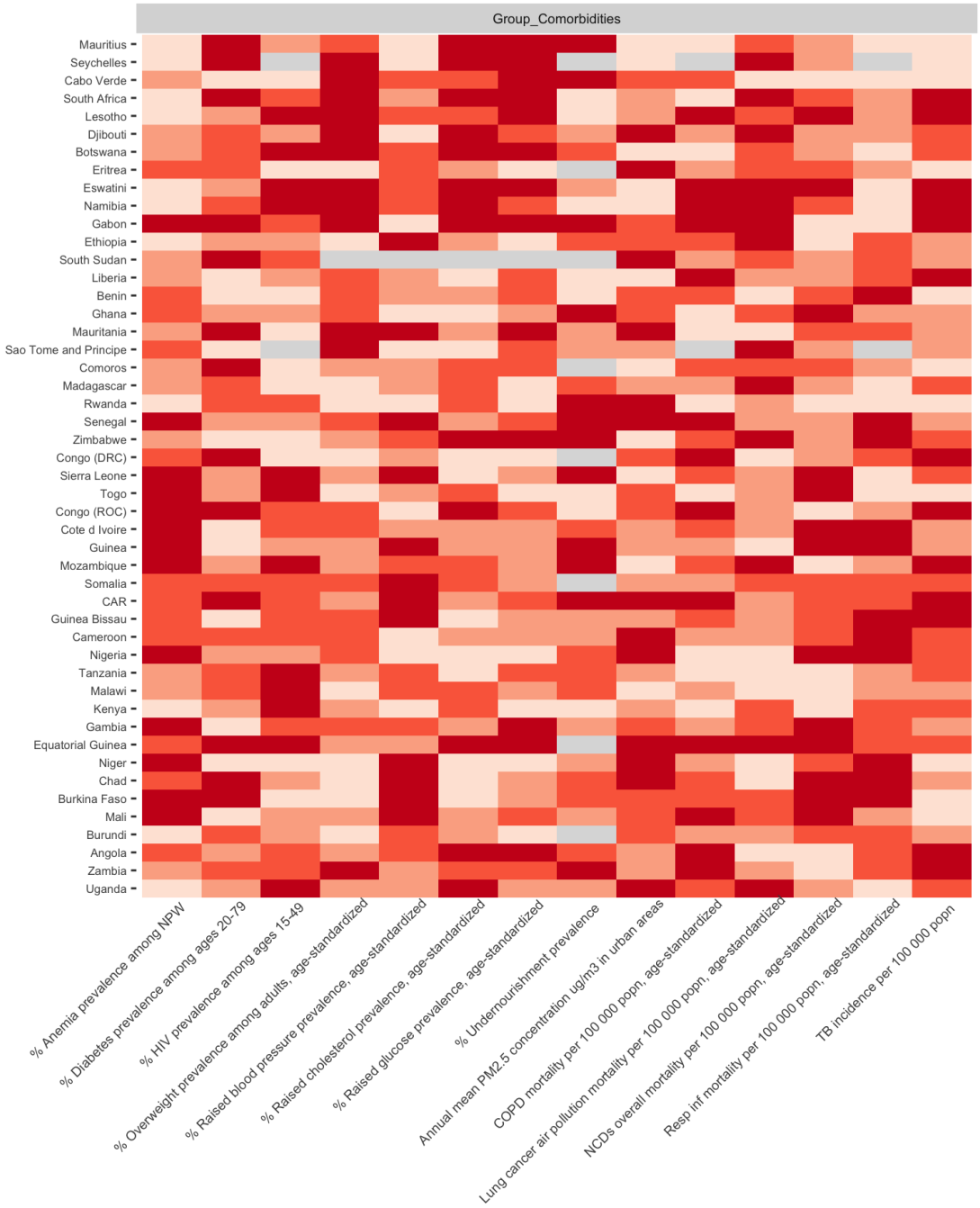

192 **B**: Select national level indicators; estimates of reduced access to care (e.g., fewer hospitals) shown with darker red
193 for higher risk quartiles Countries missing data for an indicator (NA) are shown in gray. For comparison between
194 countries, estimates are age-standardized where applicable (see **Table S3** for details)

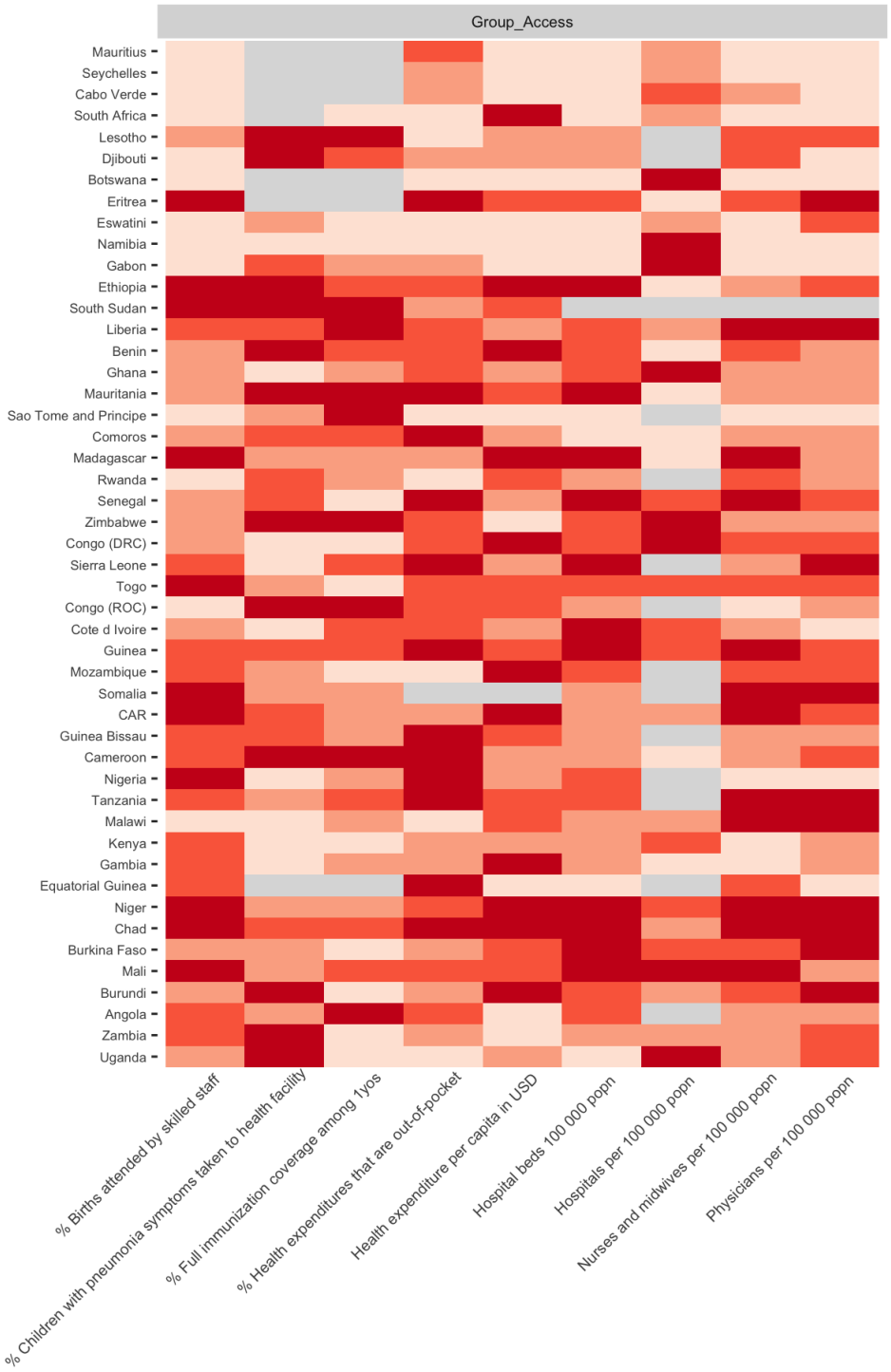

195

A3 | Principal component analysis (PCA) of variables considered

3.1 Selection of data and variables

The 29 national level variables from **Table S3** were selected for principal component analysis (PCA). We conducted further PCA on the subset of eight indicators related to access to healthcare (Category E) and the 14 national indicators variables related to comorbidities (Category B).

We excluded disaggregated sub-national spatial variation data (variables A2, C1, E2, and Category F), disaggregated or redundant variables derived from already included variables (variables A4 and D2), and disaggregated age-specific disease data from IHME global burden of disease study (variables B2, B4, and B13) from PCA analysis. COVID-19 tests per 100,000 population (variable D4, **Table S1**), per capita gross domestic product (GDP) (Variable A8), and the GINI index of wealth inequality (Variable A9) were used to visualize patterns among sub-Saharan Africa countries.

In some cases, data were missing for a country for an indicator; in these cases, missing data were replaced with a zero value. This is a conservative approach as zero values (i.e., outside the range of typical values seen in the data) inflate the total variance in the data set and thus, if anything, deflate the percent of the variance explained by PCA. Therefore, this approach avoids mistakenly attributing predictive value to principal components due to incomplete data. See **Table S3** for data sources for each variable.

3.2 Principal Component Analysis

The PCA was conducted on each of the three subsets described above, using the scikitlearn library [64]. In order to avoid biasing the PCA due to large differences in magnitude and scale, each feature was centered around the mean, and scaled to unit variance prior to the analysis. Briefly, PCA applies a linear transformation to a set of *n* features to output a set of *n* orthogonal principal components which are uncorrelated and each explain a percentage of the total variance in the dataset [65]. A link to the code for this analysis is available online at the shiny app [SSA-SARS-CoV-2-tool].

The principal components were then analyzed for the percentage of variance explained, and compared to: (i) the number of COVID-19 tests per 100,000 population as of the end of June, 2020 (**Table S1**), (ii) the per capita GDP, and (iii) the GINI index of wealth inequality. For the GINI index, estimates from 2008-2018 were available for 45 of the 48 countries (no GINI index data were available for Eritrea, Equatorial Guinea, and Somalia) (see **Data File 1** for the year for each country for each metric).

3.3 PCA Results

The first two principal components from the analysis of 29 variables explain 32.6%, and 13.1% the total variance, respectively, in the dataset. Countries with higher numbers of completed SARS-CoV-2 tests reported tended to associate with an increase in principal component 1 (Pearson correlation coefficient, $r = 0.67$, $p = 1.1e-7$, **Figure S5A**). Similarly, high GDP countries seem to associate with an increase in principal component 1 (Pearson correlation coefficient, $r = 0.80$, $p = 6.02e-12$), **Figure S5B**). In contrast, countries with greater wealth inequality (as measured by the GINI index) are associated with a decrease in principal component 2 (Pearson correlation coefficient, $r = -0.42$, $p = .0042$, **Figure S5C**). Despite these correlations, a relatively low percentage of variance is explained by each principal component: for the 29 variables, 13 of the 29 principal components are required to explain 90% of the variance (**Figure S5D**). When only the access to care subset of variables is considered, the first two principal components explain 50.7% and 19.1% of the variance, respectively, and five of eight principal components are required to explain 90% of the variance. When only the comorbidities subset is considered, the first two principal components explain 27.9% and 17.8% of the variance, respectively, and nine of 14 principal components are required to explain 90% of the variance (**Figure S4D**).

3.4 PCA Discussion

These data suggest that inter-country variation in this dataset is not easily explained by a small number of variables. Moreover, though correlations exist between principal components and high-level explanatory variables (testing capacity, wealth), their magnitude is modest. These results highlight that dimensionality reduction is unlikely to be an effective analysis strategy for the variables considered in this study. Despite this overall finding, the PCA on the access to care subset of variables highlights that the variance in these variables is more easily explained by a small number of principal components, and hence may be more amenable to dimensionality reduction. This finding is unsurprising as, for example, the number of hospital beds per 100,000 population is likely to be directly related to the number of hospitals per 100,000 population (indeed $r = 0.60$, $p = 5.7e-6$ for SSA). In contrast, for comorbidities, the relationship between different variables is less clear. Given the low percentages of variation captured by each principal component, and the high variability between different types of variables, these results motivate a holistic approach to using these data for assessing relative SARS-CoV-2 risk across SSA.

Figure S5

Principal Component Analysis of all variables and category specific subsets of variables

A: Principal Component 1 and 2, countries colored by Log10 scaled tests per 100,000 population (as of June 30, 2020)

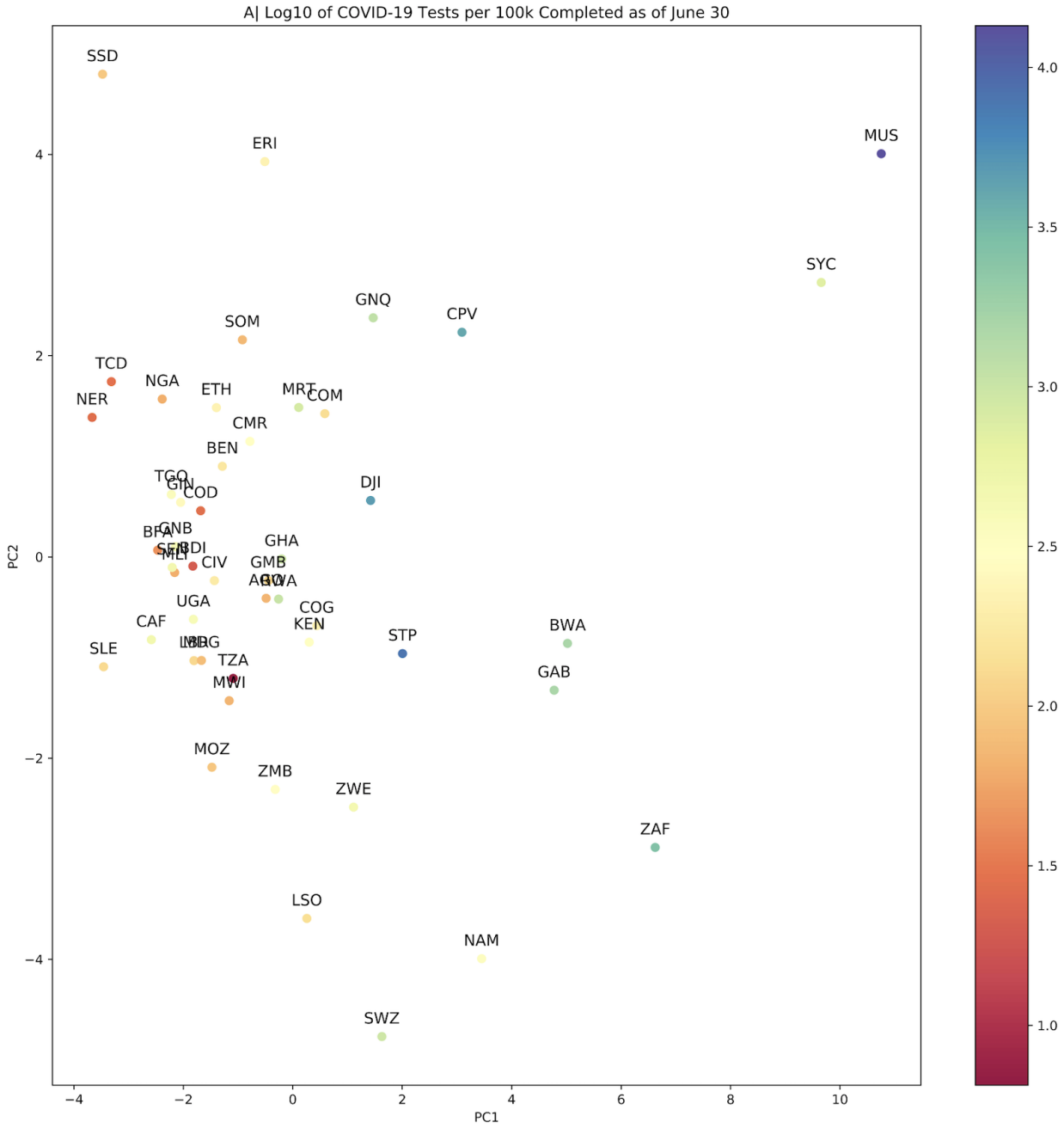

(Figure S5 continued)

Figure S5

Principal Component Analysis of all variables and category specific subsets of variables

B: Principal Component 1 and 2, countries colored by Log10 scaled GDP per capita

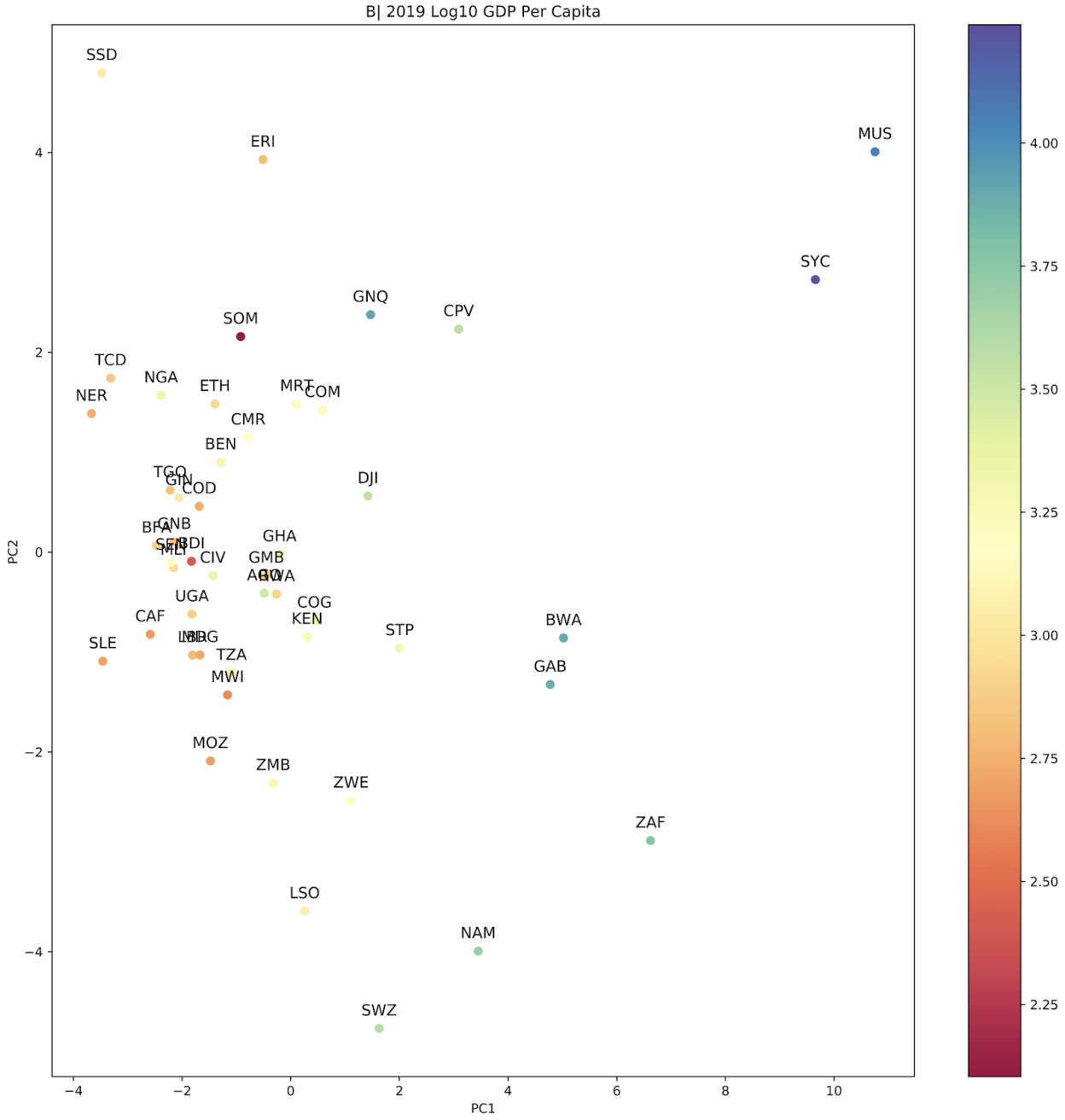

(Figure S5 continued)

Figure S5

Principal Component Analysis of all variables and category specific subsets of variables

C: Principal Component 1 and 2, countries colored by the GINI index (a measure of wealth disparity)

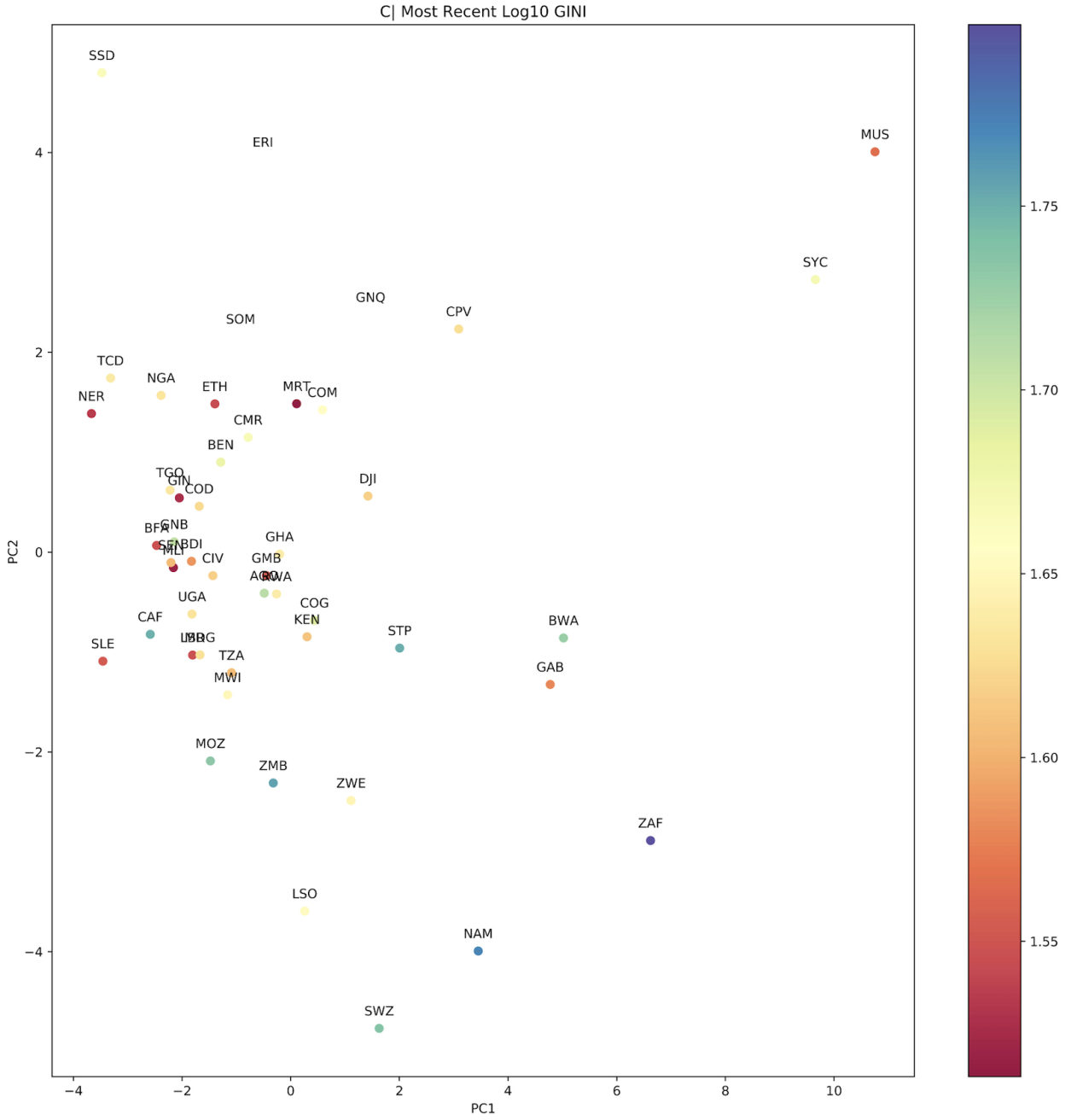

(Figure S5 continued)

Figure S5

Principal Component Analysis of all variables and category specific subsets of variables

D: Scree plot showing the cumulative proportion of variance explained by principal component for analysis done using all variables (blue, 29 variables), comorbidity indicators (green, 8 variables, Section B in **Table S3**)), and access to care indicators (orange, 14 variables, Section E in **Table S3**)

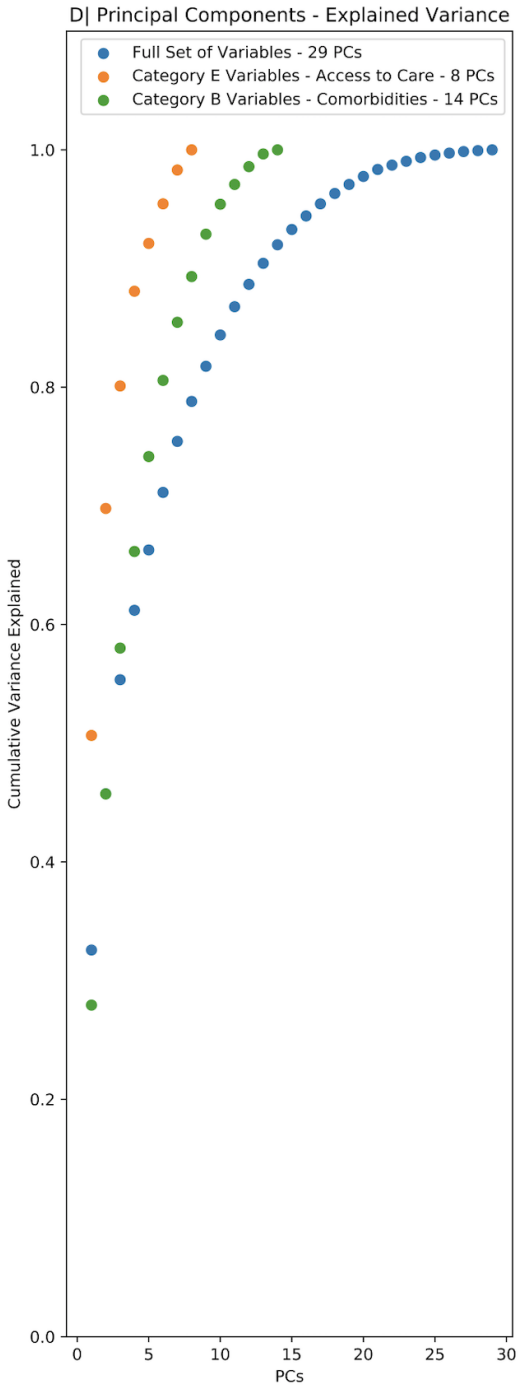

A4 | Evaluating the burden emerging from the severity of infection outcome

4.1 Data sourcing: Empirical estimates of IFR

Estimates of the infection fatality ratio (*IFR*) that account for asymptomatic cases, underreporting, and delays in reporting are few, however, it is evident that *IFR* increases substantially with age [66]. We use age-stratified estimates of *IFR* from three studies (two published [2,4], one preprint [3]) that accounted for these factors in their estimation (**Table S4**).

Table S4: Sources of age-stratified IFR estimates

Study	Population	Methods
Salje et al. 2020 [2]	Deaths and hospitalizations due to COVID-19 in French public and private hospitals across the country between 13 March - 11 May	Combined data from France with data from Diamond Princess Cruise ship to estimate age-stratified IFR, case severity, and hospitalization probabilities accounting for asymptomatic cases and underascertainment.
Verity et al. 2020 [4]	Deaths due to COVID-19 in Hubei province, China	Combined data from Hubei with data from PCR testing of repatriated citizens under quarantine to estimate age-stratified IFR accounting for asymptomatic cases and underascertainment.
Rinaldi et al. 2020 [3]	Deaths due to COVID-19 reported in Lombardia, Italy	Analyzed deaths in the Lombardia region, one of the hardest hit regions in Italy, and used seroprevalence surveys of the region to estimate that 30% of the population was infected to estimate age-stratified IFR.

To apply these estimates to other age-stratified data with different bin ranges and generate continuous predictions of *IFR* with age, we fit the relationship between the midpoint of the age bracket and the *IFR* estimate using a generalized additive model (GAM) using the ‘mgcv` package [67] in R version 4.0.2 [68]. We use a beta distribution as the link function for IFR estimates (data distributed on [0, 1]). For the upper age bracket (80+ years), we take the upper range to be 100 years and the midpoint to be 90.

We assume a given level of cumulative infection (here 20% in each age class, i.e., a constant rate of infection among age classes) and then apply *IFRs* by age to the population structure of each country to generate estimates of burden. Age structure estimates were taken from the UNPOP (see **Table S3**) country level estimates of population in 1 year age groups (0 - 100 years of age) to generate estimates of burden.

331 *4.2 Data sourcing: Comorbidities over age from IHME*
332
333 Applying these *IFR* estimates to the demographic structure of SSA countries provides a
334 baseline expectation for mortality, but depends on the assumption that mortality patterns in sub-
335 Saharan Africa will be similar to those from where the *IFR* estimates were sourced (France,
336 China, and Italy). Comorbidities have been shown to be an important determinant of the severity
337 of infection outcomes (i.e., *IFR*); to assess the relative risk of comorbidities across age in SSA,
338 estimates of comorbidity severity by age (in terms of annual deaths attributable) were obtained
339 from the Institute for Health Metrics and Evaluation (IHME) Global Burden of Disease (GBD)
340 study in 2017 [69]. Data were accessed through the GBD results tool for cardiovascular disease,
341 chronic respiratory disease (not including asthma), and diabetes, reflecting three categories of
342 comorbidity with demonstrated associations with risk (**Table S2**). We make the assumption that
343 higher mortality rates due to these NCDs, especially among younger age groups, is indicative of
344 increased severity and lesser access to sufficient care for these diseases - suggesting an
345 elevated risk for their interaction with SARS-CoV-2 as comorbidities. While there are significant
346 uncertainties in these data, they provide the best estimates of age specific risks and have been
347 used previously to estimate populations at risk[18].
348
349 The comorbidity by age curves for SSA countries were compared to those for the three
350 countries from which SARS-CoV-2 *IFR* by age estimates were sourced. Attributable mortality
351 due to all three NCD categories is higher at age 50 in all 48 SSA countries when compared to
352 estimates from France and Italy and for 42 of 48 SSA countries when compared to China
353 (**Figure S5**).
354
355 Given the potential for populations in SSA to experience a differing burden of SARS-CoV-2 due
356 to their increased severity of comorbidities in younger age groups, we explore the effects of
357 shifting *IFRs* estimated by the GAM of *IFR* estimates from France, Italy, and China younger by
358 2, 5, and 10 years (**Figure 3** in main text).
359
360

Figure S6

Comorbidity burden by age in sub-Saharan Africa

Estimated mortality per age group for sub-Saharan African countries (gray lines) compared to China, France, and Italy (the countries from which estimates of SARS-CoV-2 infection fatality ratios (*IFR*s) by age are available) for three NCD categories (cardiovascular diseases, chronic respiratory diseases excluding asthma, and diabetes).

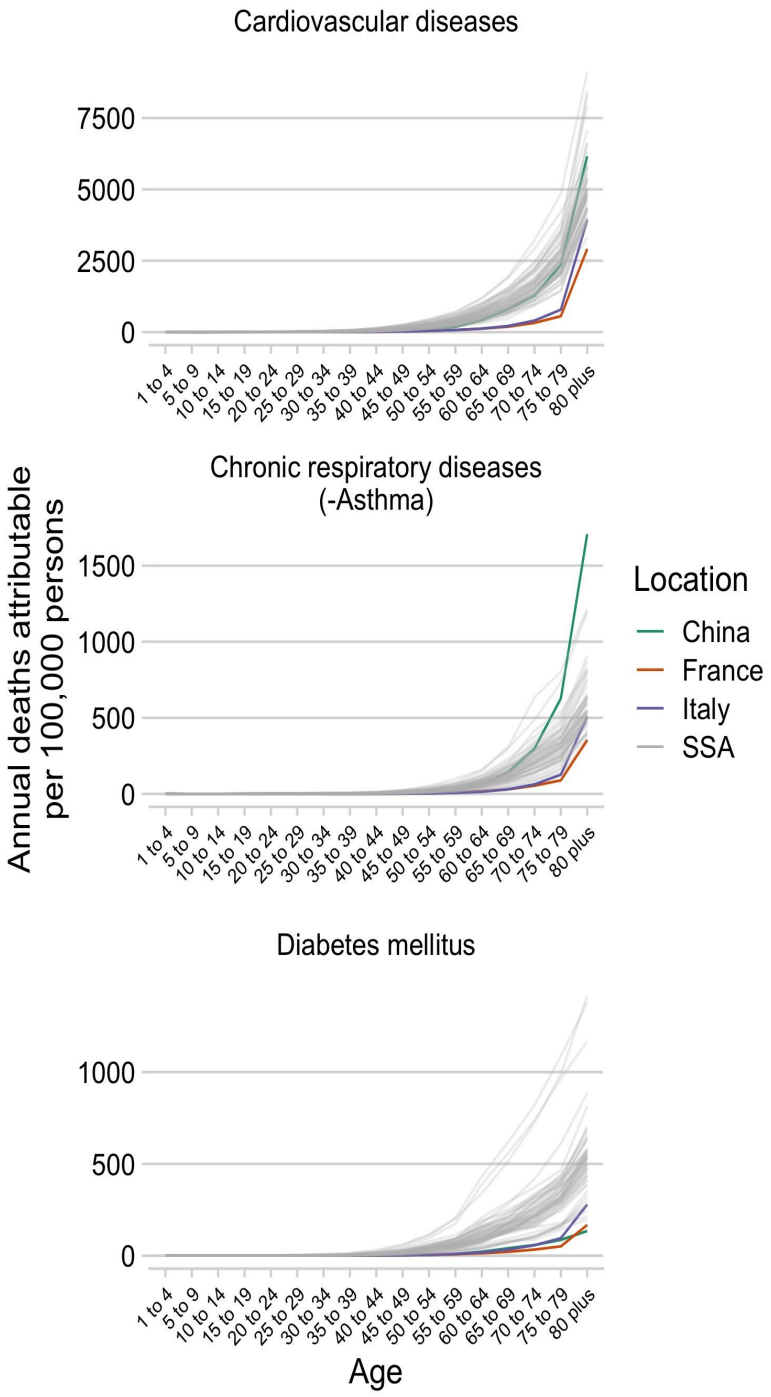

A5 | International Air Travel to SSA

The number of passenger seats on flights arriving to international airports were grouped by country and month for January 2020 to April 2020 (**Table S5**) - the months when the introduction of SARS-CoV-2 to SSA countries was likely to have first occurred. The first confirmed case reported from a SSA country, per the Johns Hopkins Coronavirus Research Center was in Nigeria on February 28, 2020. By March 31, 2020, 43 of 48 SSA countries had reported SARS-CoV-2 infections and international travel was largely restricted by April. Lesotho was the last SSA country to report a confirmed SARS-CoV-2 infection (on May 13, 2020); however, given difficulties in surveillance, the first reported detections were likely delayed relative to the first importations of the virus.

The probability of importation of the virus is defined by the number of travelers from each source location each date and the probability that a traveler from that source location on that date was infectious. Due to limitations in surveillance, especially early in the SARS-CoV-2 pandemic, empirical data on infection rates among travelers is largely lacking. To account for differences in the status of the SARS-CoV-2 pandemic across source locations, and thus differences in the importation risk for travelers from those locations, we coarsely stratified travelers arriving each day into four categories based on the status of their source countries:

i. Travelers from countries with zero reported cases (i.e., although undetected transmission was possibly occurring, SARS-CoV had not yet been confirmed in the source country by that date)
ii. Those traveling from countries with more than one reported case (i.e., SARS-CoV-2 had been confirmed to be present in that source country by that date),
iii. Those traveling from countries with more than 100 reported cases (indicating community transmission was likely beginning), and
iv. Those traveling from countries with more than 1000 reported cases (indicating widespread transmission)

For determining reported case counts at source locations for travelers, no cases were reported outside of China until January 13, 2020 (the date of the first reported case in Thailand). Over January 13 to January 21, cases were then reported in Japan, South Korea, Taiwan, Hong Kong, and the United States (https://covid19.who.int/). Subsequently, counts per country were tabulated daily by the Johns Hopkins Coronavirus Resource Center [70] beginning January 22 (https://coronavirus.jhu.edu/map.html); we use that data from January 22 onwards and the WHO reports prior to January 22.

The number of travelers within each category arriving per month is shown in **Table S5**. This approach makes the conservative assumption that the probability a traveler is infected reflects the general countrywide infection rate of the source country at the time of travel (i.e., travelers are not more likely to be exposed than non-travelers in that source location) and does not account for complex travel itineraries (i.e., a traveler from a high risk source location transiting

through a low risk source location would be grouped with other travelers from the low risk source location). Consequently, the risk for viral importation is likely systematically underestimated. However, as the relative risk for viral importation will still scale with the number of travelers, comparisons among SSA countries can be informative (e.g., SSA countries with more travelers from countries with confirmed SARS-CoV-2 transmission are at higher risk for viral importation).

Table S5

Arrivals to SSA airports by the number of passenger seats and status of the SARS-CoV-2 pandemic at the origin at the time of travel

(attached as a csv file: “Table S5 International Airtravel to SSA.csv”)

Data Fields:

1. country: Name of country
2. n_airports: Number of airports with flight data
3. month: January, February, March, April 2020; or total for all 4 months
4. total_n_seats: Total number of passenger seats on arriving aircraft
5. From source with cases > 0: Number of passengers arriving from source locations with 1 or more reported SARS-CoV-2 infection by the date of travel
6. From source with cases > 100: Number of passengers arriving from source locations more than 100 reported SARS-CoV-2 infection by the date of travel
7. From source with cases > 1000: Number of passengers arriving from source locations with more than 1000 reported SARS-CoV-2 infection by the date of travel

A6 | Subnational connectivity among countries in sub-Saharan Africa

6.1. Indicators of subnational connectivity

To allow comparison of the relative connectivity across countries, we use the friction surface estimates provided by Weiss et al.[24] as a relative measure of the rate of human movement between subregions of a country. For connectivity within subregions of a country (e.g., transport from a city to the rural periphery), we use as an indicator the population weighted mean travel time to the nearest urban center (i.e., population density > 1,500 per square kilometer or a density of built-up areas > 50% coincident with population > 50,000) within administrative-2 units [63]. For some countries, estimates at administrative-2 units were unavailable (Comoros, Cape Verde, Lesotho, Mauritius, Mayotte, and Seychelles); estimates at the administrative-1 unit level were used for these cases (these were all island nations, with the exception of Lesotho).

6.2. Metapopulation model methods

Once SARS-CoV-2 has been introduced into a country, the degree of spread of the infection within the country will be governed by subnational mobility: the pathogen is more likely to be introduced into a location where individuals arrive more frequently than one where incoming travellers are less frequent. Large-scale consistent measures of mobility remain rare. However, recently, estimates of accessibility have been produced at a global scale [24]. Although this is unlikely to perfectly reflect mobility within countries, especially as interventions and travel restrictions are put in place, it provides a starting point for evaluating the role of human mobility in shaping the outbreak pace across SSA. We use the inverse of a measure of the cost of travel between the centroids of administrative level 2 spatial units to describe mobility between locations (estimated by applying the costDistance function in the *gdistance* package in R to the friction surfaces supplied in ref[24]). With this, we develop a metapopulation model for each country to develop an overview of the possible range of trajectories of unchecked spread of SARS-CoV-2.

We assume that the pathogen first arrives into each country in the administrative 2 level unit with the largest population (e.g., the largest city) and the population in each administrative 2 level (of size N_j) is entirely susceptible at the time of arrival. We then track spread within and between each of the administrative 2 level units of each country. Within each administrative 2 level unit, dynamics are governed by a discrete time Susceptible (S), Infected (I) and Recovered (R) model with a time-step of ~ 1 week, which is broadly consistent with the serial interval of SARS-CoV-2. Within the spatial unit indexed *j*, with total size N_j, dynamics follow:

$$I_{j,t+1} = \beta {I^{\alpha}}_{j,t} S_{j,t}/N_j + \iota_{j,t}$$
$$S_{j,t+1} = S_{j,t} - I_{j,t+1} + b$$

where β captures the magnitude of transmission over the course of one serial interval (and is set to 2.5 to approximately represent the R_0 of SARS-CoV-2); the exponent $\alpha = 0.97$ is used to capture the effects of discretization[71], $\iota_{j,t}$ captures the introduction of new infections into site *j* at time *t*, and b reflects the introduction of new susceptible individuals resulting from the birth rate, set to reflect the most recent estimates for that country from the World Bank Data Bank (https://data.worldbank.org/indicator/SP.DYN.CBRT.IN).

We make the simplifying assumption that mobility linking locations *i* and *j*, denoted $c_{i,j}$, scales with the inverse of the cost of travel between sites *i* and *j* evaluated according to the friction surface provided in [24]. The introduction of an infected individual into location *j* is then defined by a draw from a Bernouilli distribution following:

$$\iota_{j,t} \sim Bern(1 - exp(-\sum_{1}^{L} c_{i,j} I_{i,t}/N_i))$$

where *L* is the total number of administrative 2 units in that country, and the rate of introduction is the product of connectivity between the focal location and each other location multiplied by the proportion of population in each other location that is infected.

Some countries show rapid spread between administrative units within the country (e.g., a country with parameters that broadly reflect those available for Malawi, **Figure S7**), while in others (e.g., reflecting Madagascar), connectivity may be so low that the outbreak may be over in the administrative unit of the largest size (where it was introduced) before introductions successfully reach other poorly connected administrative units. The result is a hump shaped relationship between the fraction of the population that is infected after 5 years and the time to the first local extinction of the pathogen (**Figure S7**, right top). In countries with lower connectivity (e.g., that might resemble Madagascar), local outbreaks can go extinct rapidly before travelling very far; in other countries (e.g., that might resemble Gabon), the pathogen goes extinct rapidly because it travels rapidly and rapidly depletes susceptible individuals everywhere.

The impact of the pattern of travel between centroids is echoed by the pattern of travel within administrative districts: countries where the pathogen does not reach a large fraction of the administrative 2 units within the country in 5 years are also those where within administrative unit travel is low (**Figure S7**, right bottom).

These simulations provide a window onto qualitative patterns expected for subnational spread of the pandemic virus, but there is no clear way of calibrating the absolute rate of travel between regions of relevance for SARS-CoV-2. Thus, the time-scales of these simulations should be considered in relative, rather than absolute terms. Variation in lockdown effectiveness, or other changes in mobility for a given country may also compromise relative comparisons. Variability in case reporting complicates clarifying this (**Figure S8**).

Figure S7

Pace of the outbreak

Each grey line on the left hand panels indicates the total infected across all administrative units in a metapopulation simulation with parameters reflecting the country indicated by the plot title, assuming interventions are constant. Increases after the first peak indicate the pathogen reaching a new administrative 2 unit. In Malawi-like settings (higher connectivity), more administrative units are reached rapidly, whereas in Madagascar-like settings (lower connectivity), a lower proportion of the administrative units are reached by a given time, as fewer introductions occur before the outbreak has burned out in the administrative 2 unit with the largest population. More generally, rapid disappearance of the outbreak (top right hand plot, y axis shows time to extinction) could either indicate rapid spread with a high proportion of the countries' population reached (top right hand plot, x axis) or slow spread, with many administrative units unreached, and therefore remaining susceptible. The pattern of between-administrative unit travel also echoes travel time within administrative units (lower panel, right hand side, x axis indicates fraction of administrative units unreached, and upper panel indicates travel time in hours to the nearest city of 50,000 or more people).

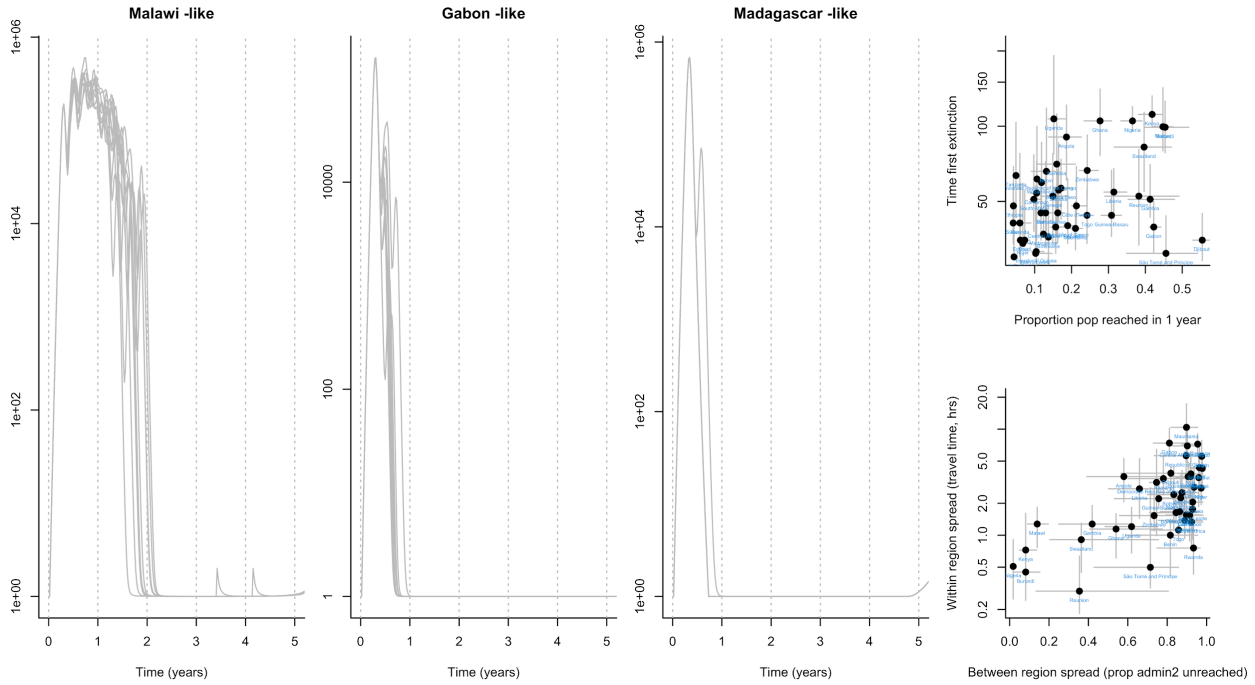

Figure S8

Cases and testing vs. the pace of the outbreak

The total number of confirmed cases reported by country (x axis, left, as reported for June 28th by Africa CDC) and the test positivity (x axis, right, defined as the total number of confirmed cases divided by the number of tests run, as reported by Africa CDC, likewise) show no significant relationship with the proportion of the population estimated to be infected after one year using the metapopulation simulation described in A6 (respectively,$\rho = -0.04, p > 0.5, df = 41$ and $\rho = 0.02, p > 0.5, df = 41$). All else equal, a positive relationship is expected; however, both uncertainty in case numbers, and uncertainty associated with the simulation might both drive the absence of a signal.

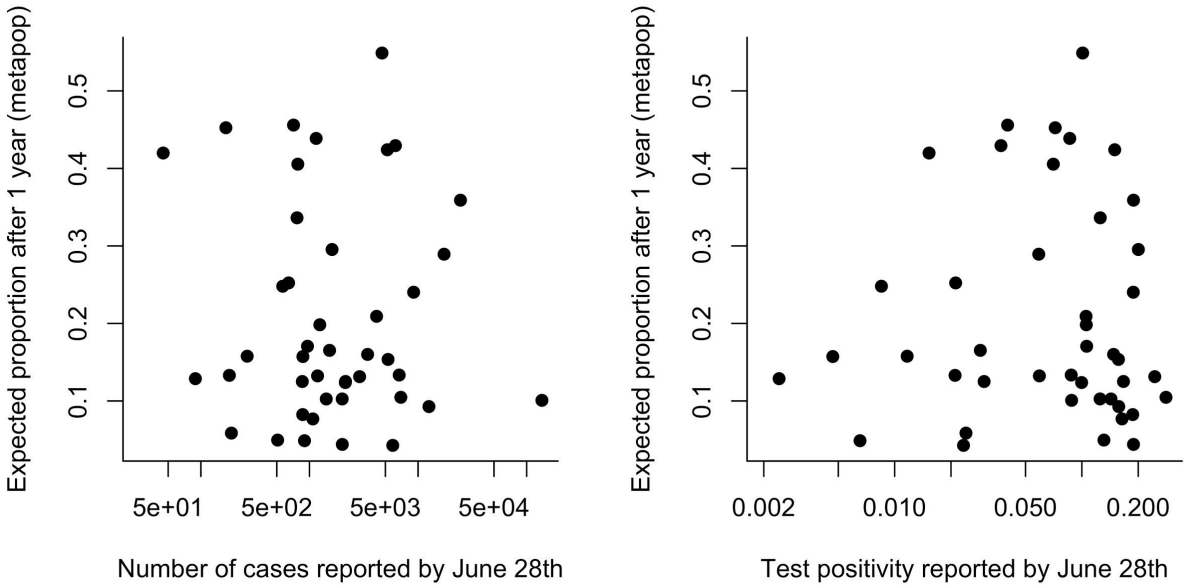

A7 | Modeling epidemic trajectories in scenarios where transmission rate depends on climate

7.1 Climate data sourcing: Variation in humidity in SSA

Specific humidity data for selected urban centers comes from ERA5 using an average climatology (1981-2017)[47]; we do not consider year-to-year climate variations. Selected cities (*n* = 58) were chosen to represent the major urban areas in SSA. The largest city in each SSA country was included as well as any additional cities that were among the 25 largest cities or busiest airports in SSA.

7.2 Methods for climate driven modelling of SARS-CoV-2

We use a climate-driven SIRS (Susceptible-Infected-Recovered-Susceptible) model to estimate epidemic trajectories (i.e., the time of peak incidence) in different cities in 2020, assuming no control measures are in place [23,72]. The model is given by:

$$\frac{dS}{dt} = \frac{N - S - L}{L} - \frac{\beta(t)IS}{N}$$

$$\frac{dI}{dt} = \frac{\beta(t)IS}{N} - \frac{I}{D}$$

where *S* is the susceptible population, *I* is the infected population and *N* is the total population. *D* is the mean infectious period, set at 5 days following ref[23,49]. To investigate the maximum possible climate effect, we use parameters from the most climate-dependent scenario in ref[23], based on betacoronavirus HKU1. In this scenario *L*, the duration of immunity, is found to be 66.25 weeks (i.e., greater than 1 year and such that waning immunity does not affect timing of the epidemic peak).

Transmission is governed by $\beta(t)$ which is related to the basic reproduction number R_0 by $R_0(t) = \beta(t)D$. The basic reproduction number varies based on the climate and is related to specific humidity according to the equation:

$$R_0 = exp\ (a * q(t) + log\ (R_{0max} - R_{0min}\ )\ ) + R_{0min}$$

where *q(t)* is specific humidity [47] and *a* is set at -227.5 based on estimated HKU1 parameters [23]. R_{0max} and R_{0min} are 2.5 and 1.5 respectively. We assume the same time of introduction for all cities, set at March 1st, 2020 (consistent with the first reported cases in SSA, **Figure S1D**)

592 **References**

593 1. Mecenas, P., Bastos, R., Vallinoto, A. & Normando, D. Effects of temperature and humidity
594 on the spread of COVID-19: A systematic review. doi:10.1101/2020.04.14.20064923.
595 2. Salje, H. *et al.* Estimating the burden of SARS-CoV-2 in France. *Science* (2020)
596 doi:10.1126/science.abc3517.
597 3. Rinaldi, G. & Paradisi, M. An empirical estimate of the infection fatality rate of COVID-19
598 from the first Italian outbreak. doi:10.1101/2020.04.18.20070912.
599 4. Verity, R. *et al.* Estimates of the severity of coronavirus disease 2019: a model-based
600 analysis. *Lancet Infect. Dis.* **20**, 669–677 (2020).
601 5. Africa CDC - COVID-19 Daily Updates. *Africa CDC* https://africacdc.org/covid-19/.
602 6. Mortality Analyses. *Johns Hopkins Coronavirus Resource Center*
603 https://coronavirus.jhu.edu/data/mortality.
604 7. Skrip, L. A. *et al.* Seeding COVID-19 across sub-Saharan Africa: an analysis of reported
605 importation events across 40 countries. doi:10.1101/2020.04.01.20050203.
606 8. Deng, X. *et al.* Case fatality risk of novel coronavirus diseases 2019 in China.
607 doi:10.1101/2020.03.04.20031005.
608 9. Collaborative, T. O. *et al.* OpenSAFELY: factors associated with COVID-19-related hospital
609 death in the linked electronic health records of 17 million adult NHS patients.
610 doi:10.1101/2020.05.06.20092999.
611 10. COVID-19 significantly impacts health services for noncommunicable diseases.
612 https://www.who.int/news-room/detail/01-06-2020-covid-19-significantly-impacts-health-
613 services-for-noncommunicable-diseases.
614 11. Maintaining essential health services: operational guidance for the COVID-19 context.
615 https://www.who.int/publications/i/item/covid-19-operational-guidance-for-maintaining-
616 essential-health-services-during-an-outbreak.
617 12. Santoli, J. M. Effects of the COVID-19 Pandemic on Routine Pediatric Vaccine Ordering

618 and Administration — United States, 2020. *MMWR Morb. Mortal. Wkly. Rep.* **69**, (2020).
619 13. Roberton, T. *et al.* Early estimates of the indirect effects of the COVID-19 pandemic on
620 maternal and child mortality in low-income and middle-income countries: a modelling study.
621 *Lancet Glob Health* **8**, e901–e908 (2020).
622 14. Walker, P. G. T. *et al.* The impact of COVID-19 and strategies for mitigation and
623 suppression in low- and middle-income countries. *Science* (2020)
624 doi:10.1126/science.abc0035.
625 15. Pei, S., Kandula, S. & Shaman, J. Differential Effects of Intervention Timing on COVID-19
626 Spread in the United States. *medRxiv* (2020) doi:10.1101/2020.05.15.20103655.
627 16. Lai, S. *et al.* Assessing the effect of global travel and contact reductions to mitigate the
628 COVID-19 pandemic and resurgence. doi:10.1101/2020.06.17.20133843.
629 17. Nepomuceno, M. R. *et al.* Besides population age structure, health and other demographic
630 factors can contribute to understanding the COVID-19 burden. *Proceedings of the National*
631 *Academy of Sciences of the United States of America* vol. 117 13881–13883 (2020).
632 18. Clark, A. *et al.* Global, regional, and national estimates of the population at increased risk of
633 severe COVID-19 due to underlying health conditions in 2020: a modelling study. *Lancet*
634 *Glob Health* (2020) doi:10.1016/S2214-109X(20)30264-3.
635 19. Ghisolfi, S. *et al.* Predicted COVID-19 fatality rates based on age, sex, comorbidities, and
636 health system capacity. doi:10.1101/2020.06.05.20123489.
637 20. [No title]. https://www.imperial.ac.uk/media/imperial-college/medicine/mrc-gida/2020-05-12-
638 COVID19-Report-22.pdf.
639 21. Kapata, N. *et al.* Is Africa prepared for tackling the COVID-19 (SARS-CoV-2) epidemic.
640 Lessons from past outbreaks, ongoing pan-African public health efforts, and implications for
641 the future. *International journal of infectious diseases: IJID: official publication of the*
642 *International Society for Infectious Diseases* vol. 93 233–236 (2020).
643 22. Nachega, J. B. *et al.* From Easing Lockdowns to Scaling-Up Community-Based COVID-19

644 Screening, Testing, and Contact Tracing in Africa - Shared Approaches, Innovations, and
645 Challenges to Minimize Morbidity and Mortality. *Clin. Infect. Dis.* (2020)
646 doi:10.1093/cid/ciaa695.
647 23. Baker, R. E., Yang, W., Vecchi, G. A., Metcalf, C. J. E. & Grenfell, B. T. Susceptible supply
648 limits the role of climate in the early SARS-CoV-2 pandemic. *Science* (2020)
649 doi:10.1126/science.abc2535.
650 24. Weiss, D. J. *et al.* A global map of travel time to cities to assess inequalities in accessibility
651 in 2015. *Nature* **553**, 333–336 (2018).
652 25. Tatem, A. J. WorldPop, open data for spatial demography. *Scientific Data* vol. 4 (2017).
653 26. [No title]. https://washdata.org/sites/default/files/documents/reports/2019-05/JMP-2018-
654 core-questions-for-household-surveys.pdf.
655 27. Korevaar, H. M. *et al.* Quantifying the impact of US state non-pharmaceutical interventions
656 on COVID-19 transmission. doi:10.1101/2020.06.30.20142877.
657 28. Mikkelsen, L. *et al.* A global assessment of civil registration and vital statistics systems:
658 monitoring data quality and progress. *Lancet* **386**, 1395–1406 (2015).
659 29. Gilbert, M. *et al.* Preparedness and vulnerability of African countries against importations of
660 COVID-19: a modelling study. *Lancet* **395**, 871–877 (2020).
661 30. Haider, N. *et al.* Passengers' destinations from China: low risk of Novel Coronavirus (2019-
662 nCoV) transmission into Africa and South America. *Epidemiol. Infect.* **148**, e41 (2020).
663 31. Takahashi, S. *et al.* Reduced vaccination and the risk of measles and other childhood
664 infections post-Ebola. *Science* vol. 347 1240–1242 (2015).
665 32. Cash, R. & Patel, V. Has COVID-19 subverted global health? *Lancet* **395**, 1687–1688
666 (2020).
667 33. Adams, J. G. & Walls, R. M. Supporting the Health Care Workforce During the COVID-19
668 Global Epidemic. *JAMA* (2020) doi:10.1001/jama.2020.3972.
669 34. Kilmarx, P. H. *et al.* Ebola virus disease in health care workers--Sierra Leone, 2014.

670 *MMWR Morb. Mortal. Wkly. Rep.* **63**, 1168–1171 (2014).
671 35. Covid 19 Mauritius Dashboard. *Google Data Studio*
672 http://datastudio.google.com/reporting/510dbd29-25cd-4fbb-a47a-
673 68effeda6cf5/page/0z6JB?feature=opengraph.
674 36. Rwanda: WHO Coronavirus Disease (COVID-19) Dashboard. https://covid19.who.int.
675 37. Mina, M. J. *et al.* A Global Immunological Observatory to meet a time of pandemics. *Elife* **9**,
676 (2020).
677 38. World Population Prospects - Population Division - United Nations.
678 https://population.un.org/wpp/Download/Standard/Population/.
679 39. The Novel Coronavirus Pneumonia Emergency Response Epidemiology Team. The
680 Epidemiological Characteristics of an Outbreak of 2019 Novel Coronavirus Diseases
681 (COVID-19) — China, 2020. *CCDCW* **2**, 113–122 (2020).
682 40. Team, C. C.-19 R. *et al.* Severe Outcomes Among Patients with Coronavirus Disease 2019
683 (COVID-19) — United States, February 12–March 16, 2020. *MMWR. Morbidity and*
684 *Mortality Weekly Report* vol. 69 343–346 (2020).
685 41. Simonnet, A. *et al.* High prevalence of obesity in severe acute respiratory syndrome
686 coronavirus-2 (SARS-CoV-2) requiring invasive mechanical ventilation. *Obesity* (2020)
687 doi:10.1002/oby.22831.
688 42. Conticini, E., Frediani, B. & Caro, D. Can atmospheric pollution be considered a co-factor in
689 extremely high level of SARS-CoV-2 lethality in Northern Italy? *Environ. Pollut.* **261**, 114465
690 (2020).
691 43. Griffith, G. *et al.* Collider bias undermines our understanding of COVID-19 disease risk and
692 severity. doi:10.1101/2020.05.04.20090506.
693 44. Shankar, A. H. Nutritional Modulation of Malaria Morbidity and Mortality. *The Journal of*
694 *Infectious Diseases* vol. 182 S37–S53 (2000).
695 45. The DHS Program - Quality information to plan, monitor and improve population, health,

696 and nutrition programs. https://dhsprogram.com.

697 46. Chin, T. *et al.* U.S. county-level characteristics to inform equitable COVID-19 response.
698 *medRxiv* (2020) doi:10.1101/2020.04.08.20058248.

699 47. Hersbach, H. *et al.* The ERA5 global reanalysis. *Q.J.R. Meteorol. Soc.* **64**, 29 (2020).

700 48. Report 23 - State-level tracking of COVID-19 in the United States. *Imperial College London*
701 http://www.imperial.ac.uk/medicine/departments/school-public-health/infectious-disease-
702 epidemiology/mrc-global-infectious-disease-analysis/covid-19/report-23-united-states/.

703 49. Kissler, S. M., Tedijanto, C., Goldstein, E., Grad, Y. H. & Lipsitch, M. Projecting the
704 transmission dynamics of SARS-CoV-2 through the postpandemic period. *Science* **368**,
705 860–868 (2020).

706 50. Jiwani, S. S. & Antiporta, D. A. Inequalities in access to water and soap matter for the
707 COVID-19 response in sub-Saharan Africa. *Int. J. Equity Health* **19**, 82 (2020).

708 51. Stoler, J., Jepson, W. E. & Wutich, A. Beyond handwashing: Water insecurity undermines
709 COVID-19 response in developing areas. *J. Glob. Health* **10**, 010355 (2020).

710 52. Makoni, M. Keeping COVID-19 at bay in Africa. *Lancet Respir Med* **8**, 553–554 (2020).

711 53. Tatem, A. J. *et al.* Ranking of elimination feasibility between malaria-endemic countries.
712 *Lancet* **376**, 1579–1591 (2010).

713 54. Metcalf, C. J. E. *et al.* Transport networks and inequities in vaccination: remoteness shapes
714 measles vaccine coverage and prospects for elimination across Africa. *Epidemiol. Infect.*
715 **143**, 1457–1466 (2015).

716 55. Adepoju, P. Africa's struggle with inadequate COVID-19 testing. *The Lancet Microbe* vol. 1
717 e12 (2020).

718 56. Pindolia, D. K. *et al.* The demographics of human and malaria movement and migration
719 patterns in East Africa. *Malar. J.* **12**, 397 (2013).

720 57. Qiu, Y., Chen, X. & Shi, W. Impacts of social and economic factors on the transmission of
721 coronavirus disease (COVID-19) in China. doi:10.1101/2020.03.13.20035238.

722 58. Li, H. *et al.* Age-Dependent Risks of Incidence and Mortality of COVID-19 in Hubei
723 Province and Other Parts of China. *Front. Med.* **7**, 190 (2020).
724 59. Global Burden of Disease Study 2017 (GBD 2017) Population Estimates 1950-2017 |
725 GHDx. http://ghdx.healthdata.org/record/ihme-data/gbd-2017-population-estimates-1950-
726 2017.
727 60. Brauer, M., Zhao, J. T., Bennitt, F. B. & Stanaway, J. D. Global access to handwashing:
728 implications for COVID-19 control in low-income countries.
729 doi:10.1101/2020.04.07.20057117.
730 61. Alegana, V. A. *et al.* National and sub-national variation in patterns of febrile case
731 management in sub-Saharan Africa. *Nat. Commun.* **9**, 4994 (2018).
732 62. Murthy, S., Leligdowicz, A. & Adhikari, N. K. J. Intensive care unit capacity in low-income
733 countries: a systematic review. *PLoS One* **10**, e0116949 (2015).
734 63. Linard, C., Gilbert, M., Snow, R. W., Noor, A. M. & Tatem, A. J. Population distribution,
735 settlement patterns and accessibility across Africa in 2010. *PLoS One* **7**, e31743 (2012).
736 64. [No title]. https://dl.acm.org/doi/10.5555/1953048.2078195.
737 65. Jolliffe, I. T. & Cadima, J. Principal component analysis: a review and recent developments.
738 *Philos. Trans. A Math. Phys. Eng. Sci.* **374**, 20150202 (2016).
739 66. Meyerowitz-Katz, G. & Merone, L. A systematic review and meta-analysis of published
740 research data on COVID-19 infection-fatality rates. doi:10.1101/2020.05.03.20089854.
741 67. Wood, S. N. *Generalized Additive Models: An Introduction with R, Second Edition*. (CRC
742 Press, 2017).
743 68. R: The R Project for Statistical Computing. https://www.R-project.org/.
744 69. Global Burden of Disease Study 2017 (GBD 2017) Population Estimates 1950-2017 |
745 GHDx. http://ghdx.healthdata.org/record/ihme-data/gbd-2017-population-estimates-1950-
746 2017.
747 70. Dong, E., Du, H. & Gardner, L. An interactive web-based dashboard to track COVID-19 in

748 real time. *Lancet Infect. Dis.* **20**, 533–534 (2020).

749 71. Bjornstad, O. N., Finkenstadt, B. F. & Grenfell, B. T. Dynamics of Measles Epidemics:
750 Estimating Scaling of Transmission Rates Using a Time Series SIR Model. *Ecological*
751 *Monographs* vol. 72 169 (2002).

752 72. Shaman, J., Pitzer, V. E., Viboud, C., Grenfell, B. T. & Lipsitch, M. Absolute humidity and
753 the seasonal onset of influenza in the continental United States. *PLoS Biol.* **8**, e1000316
754 (2010).